Light Metals 2005, TMS 2005

A New High Speed Titanium Production by Subhalide Reduction Process

Osamu Takeda[1] and Toru H. Okabe[2]

[1] Graduate student,
Graduate School of Engineering,
The University of Tokyo

[2] Institute of Industrial Science,
The University of Tokyo

Excellent Material, Titanium!

Feature of Titanium

1. Light and high-strength
2. Corrosion resistance
3. Biocompatibility
4. Some titanium alloy：
   shape memory alloy
   super elasticity

Aerospace industry

Japan Aerospace Exploration Agency

Dental material

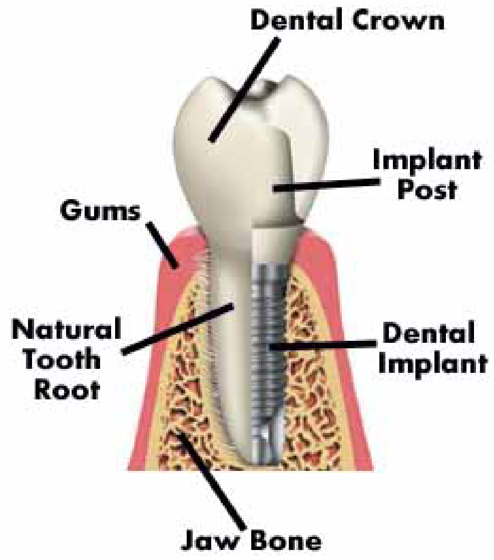

http://village.infoweb.ne.jp/~etou/indexhome.htm

Power generation plant

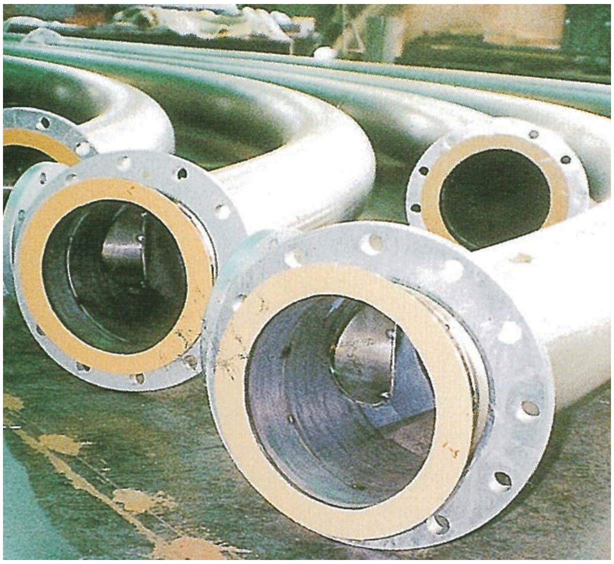

The JAPAN TITANIUM SOCIETY

Current Status of Titanium Production

(a) Production of titanium sponge in the world (2003)

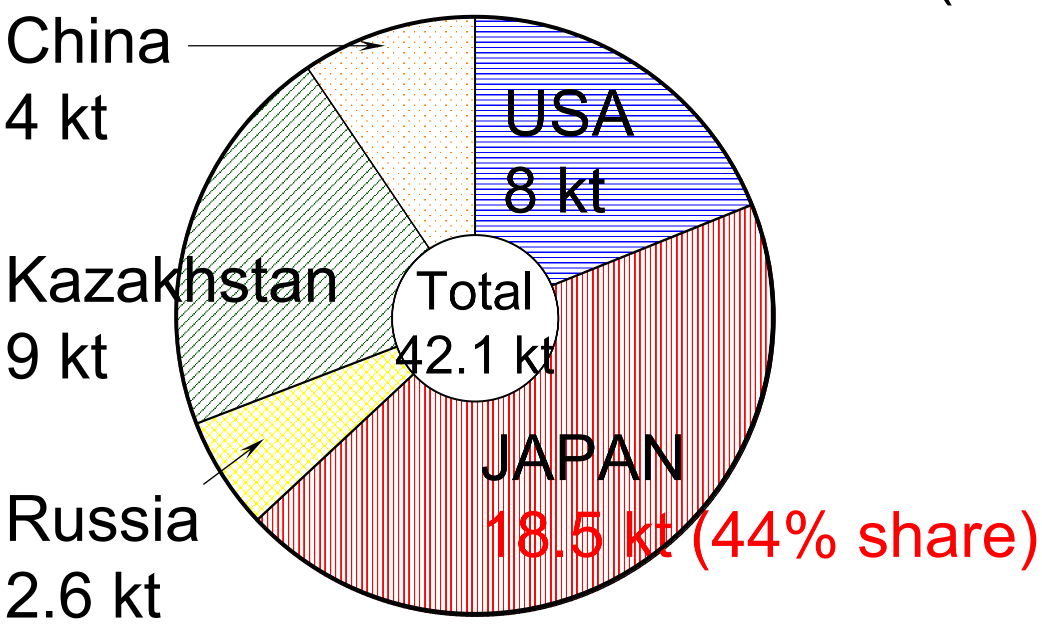

(b) Production of titanium mill products in Japan

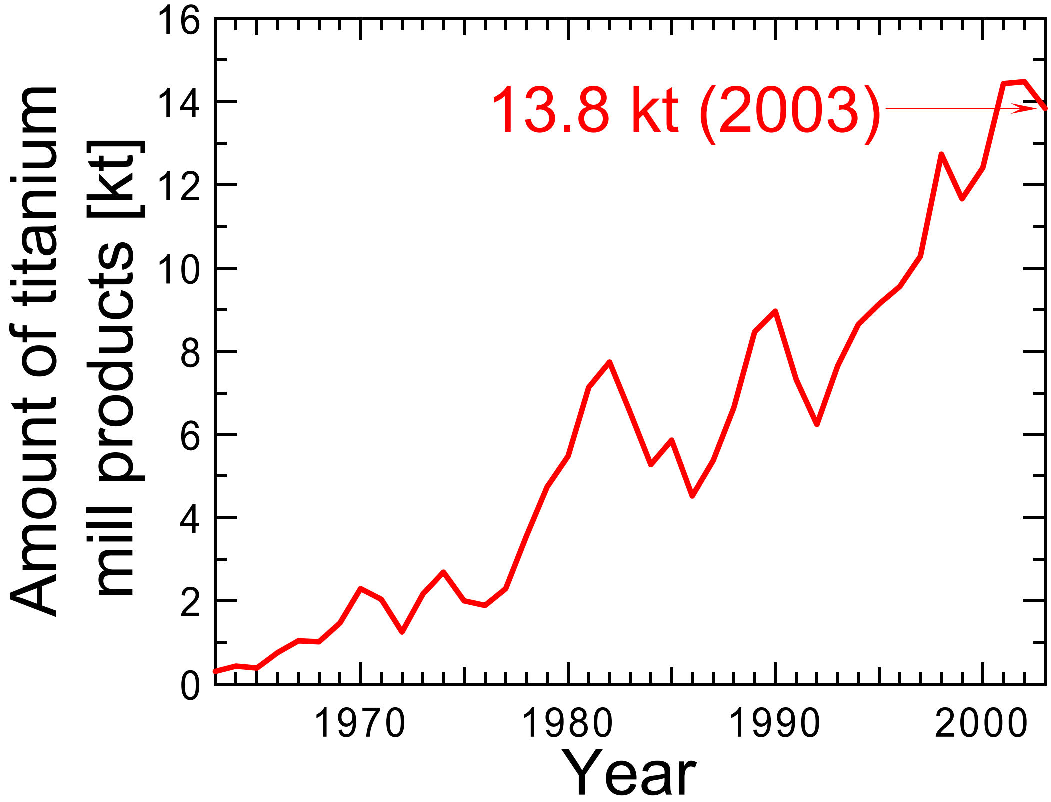

Comparison with common metals

Table
Comparison between common metals and titanium

Metal	Iron	Aluminum	Titanium
Symbol	Fe	Al	Ti
Melting point (°C)	1536	660	1680
Density (g/cm^3@25 °C)	7.9	2.7	4.5
Specific strength [$(kgf/mm^2)/(g/cm^3)$]	4.1(Pure) 6.7(SUS304)	2.2(Pure) 8.9(0.5Mg0.5Si)	5.1(Pure) 24.6(6Al4V)
Clarke No.	4	3	10
Price (¥/kg)	50	600	3000
Production volume (t/world@2003)	9.6×10^8	2.2×10^7	6.6×10^4

1/300

1/15000

Although titanium is the 10th most abundant element in the earth's crust, its production volume is very small

The Kroll Process

Chlorination: $TiO_2 + C + 2Cl_2 \rightarrow TiCl_4 + CO_2$

Reduction: $TiCl_4 + 2Mg \rightarrow Ti + 2MgCl_2$

Electrolysis: $MgCl_2 \rightarrow Mg + Cl_2$

Crushing

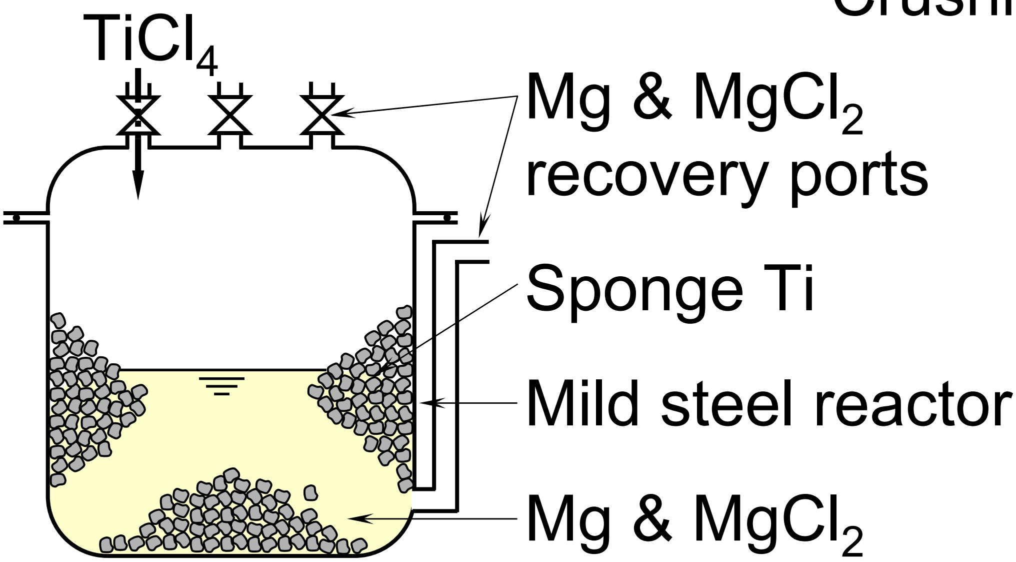

Features：

◎High-purity Ti can be obtained.

◎Metal/salt separation is easy.

○Chlorine circulation is Established.

○Efficient Mg electrolysis can be utilized.

○Reduction and electrolysis can be carried out independently.

×Process is complicated.

×Reduction process is a batch type.

×Production speed is low.

Reduction speed of Ti is <1 t/day·batch, which is one of the contributors to its high cost.

Current Status of Titanium Metallurgy

The FFC Cambridge process (2000)

↓

The direct reduction processes of titanium oxide (TiO_2) (e.g., the OS process, the EMR/MSE process, the ESR process)

$$TiO_2(s) + e^- \rightarrow Ti(s) + O^{2-} \quad \text{(in } CaCl_2\text{)}$$
$$TiO_2(s) + Ca \rightarrow Ti(s) + CaO \quad \text{(in } CaCl_2\text{)}$$

Difficulties in using TiO_2:

- Production of high-purity TiO_2 feed is expensive.
- Energy efficiency is low.
- Metal/salt separation is difficult.
- Purity control of obtained Ti is difficult.

Advantages of the Kroll process:

- Oxygen and iron removal by the chlorination process is highly efficient.
- Metal/salt separation by vacuum distillation is easy.
- High-purity Ti with low oxygen is obtainable.
- Mg and Cl_2 are reusable.

Purpose of this Study

Establishment of a continuous and high-speed titanium reduction process based on the magnesiothermic reduction of titanium chlorides

The Kroll process
Feed: $TiCl_4$
- High reduction heat
- Stability as a gas phase

→Low reduction speed to control the reactor temperature
→Long cool time for the reactor after reduction

Subhalide reduction process
Feed: Titanium subchlorides ($TiCl_x$, x = 2, 3)
- Low reduction heat
- Stability as a condensed phase

→High reduction speed

Properties of Titanium Chloride

	$TiCl_4$	$TiCl_3$	$TiCl_2$
Appearance		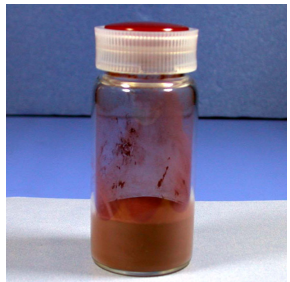	
Color	Clear	Red	Black
Molecular weight (g/mol)	189.7	154.2	118.8
Density (g/cm^3)	1.70	No data	3.13
Melting point (°C)	–24.1	–	–
Boiling point (°C)	136.5	–	–
Sublimation point (°C)	–	830	1307
ΔG°_f at 800°C (kJ/mol Cl_2)	–317	–327	–344
$\Delta G'^\circ_f$ at 800°C (kJ/mol Ti)	–637	–491	–344
Vapor pressure at 800°C (atm)	–	0.74	1.2×10^{-4}

New Titanium Production Process Using Titanium Subhalides ($TiCl_x$, x = 2, 3)

① $TiCl_4(l, g) + Mg(l, g) \rightarrow TiCl_x(s, l) + MgCl_2(l)$

$TiCl_4(l, g) + Ti(s, scrap) \rightarrow TiCl_x(s, l)$

② $TiCl_x(s, l) + Mg(l, g) \rightarrow Ti(s) + MgCl_2(l, g)$

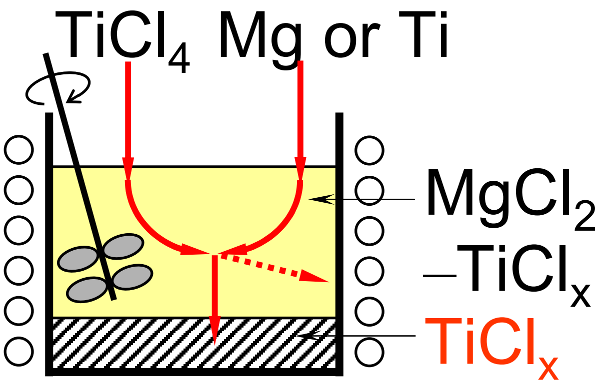

Step 1:
High-speed production of Ti subchlorides and enrichment of $TiCl_x$

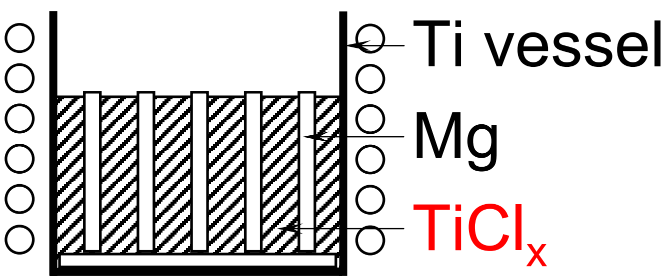

Step 2:
High-speed magnesiothermic reduction of $TiCl_x$

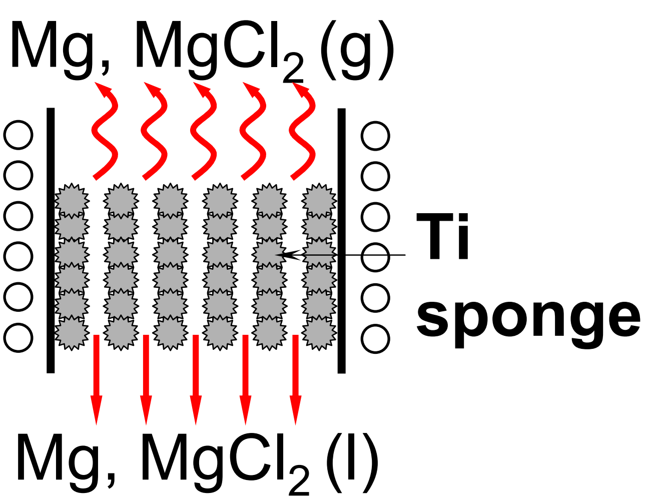

Step 3:
High-speed removal of Mg and $MgCl_2$ from Ti sponge by draining and vacuum distillation

Features of the New Process

Table
Comparison of the Kroll process and new process

	Kroll process	New process
Process type	Batch-type, limited speed	(Semi-)Continuous, high speed
Feed material	$TiCl_4$ (l, g)	$TiCl_2$ or $TiCl_3$ (s, l)
Heat of reduction, $\Delta H°$ / kJ mol Ti	High (–434)	Low (–94 ~ –191)
Reactor material	Mild steel (Iron contamination unavoidable)	Titanium (No iron contamination)
Reactor size	Large (Crush and melt)	Small (No crush and direct melt)
Flux, sealant	Not used	$MgCl_2$, Ti
Common features	• Magnesiothermic reduction of chloride • Removal of $MgCl_2$ and Mg from Ti sponge by draining and vacuum distillation • Production of high-purity Ti with low oxygen content	

Today's Report

Investigation of magnesiothermic reduction of titanium subchloride ($TiCl_x$, x = 2, 3)

Route A: $2\ TiCl_3 + 3\ Mg \rightarrow 2\ Ti + 3\ MgCl_2$

Route B: $2\ TiCl_3 + Ti \rightarrow 3\ TiCl_2$

$TiCl_2 + Mg \rightarrow Ti + MgCl_2$

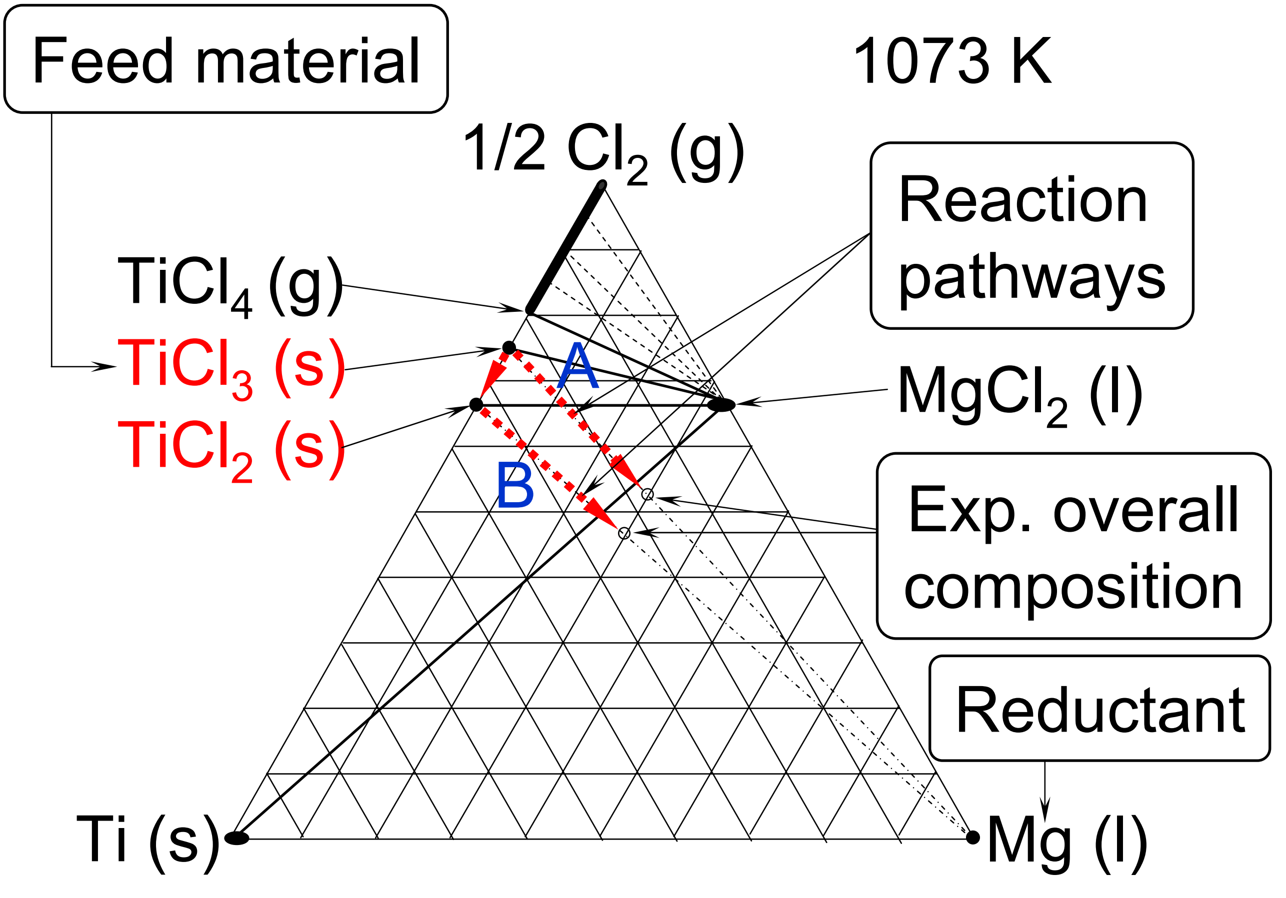

Figure Isothermal phase diagram for the Ti–Mg–Cl ternary system at 1073 K. [Ref. Okabe et al.: J. Japan Inst. Metals 61 (1997) pp. 610-618.]

Experimental Apparatus

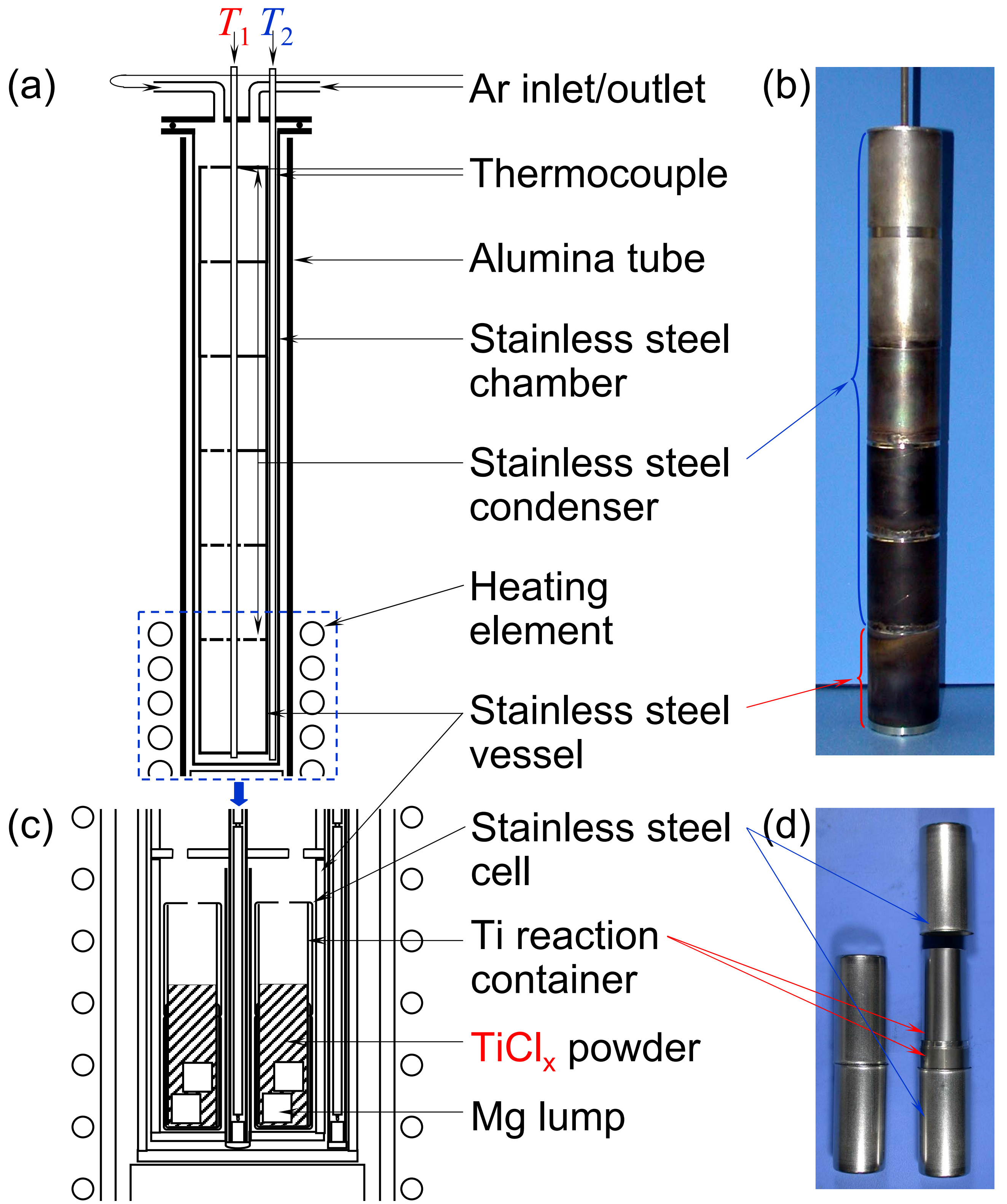

Figure Schematic illustration of the experimental apparatus for the magnesiothermic reduction of $TiCl_x$.

Results: Transition of Temperature

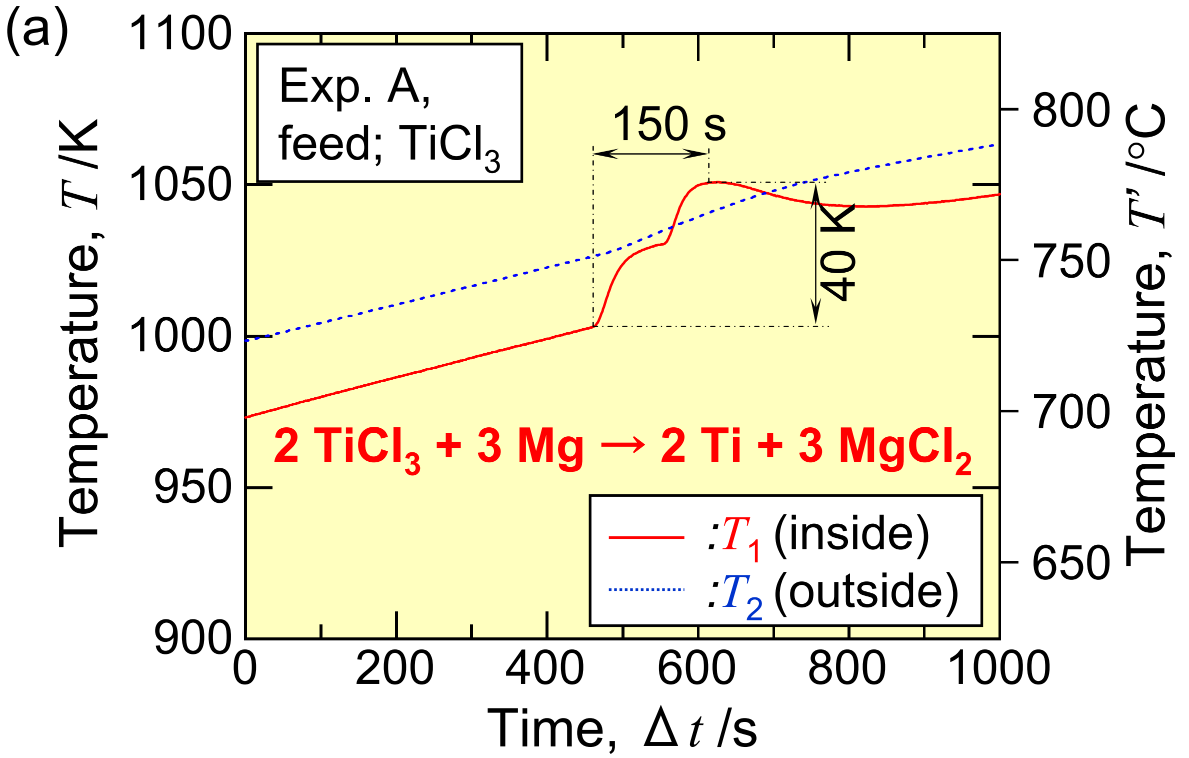

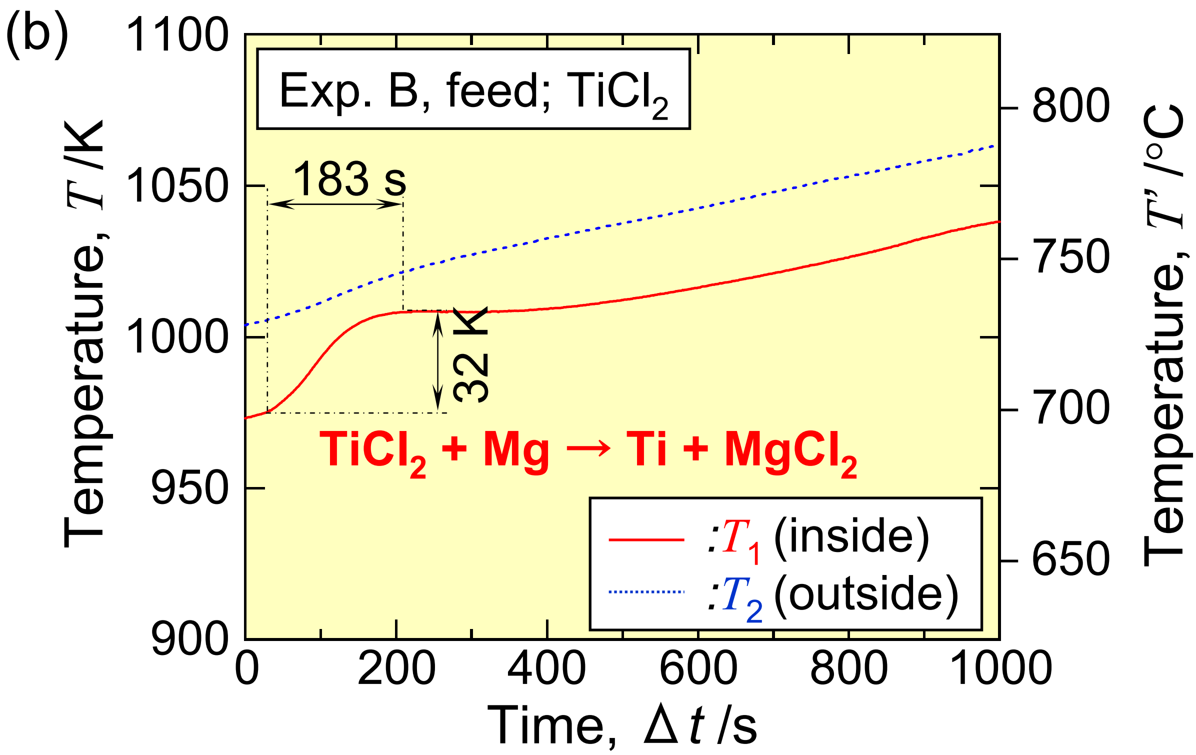

Figure Representative transition of the sample temperature during the magnesiothermic reduction. [G, R]

Results: Appearance of Sample

(a) Sectioned reaction container after reduction

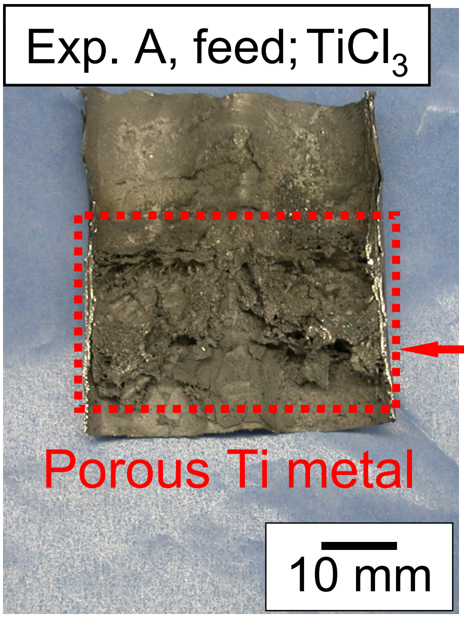

(b) Initial setup of (a)

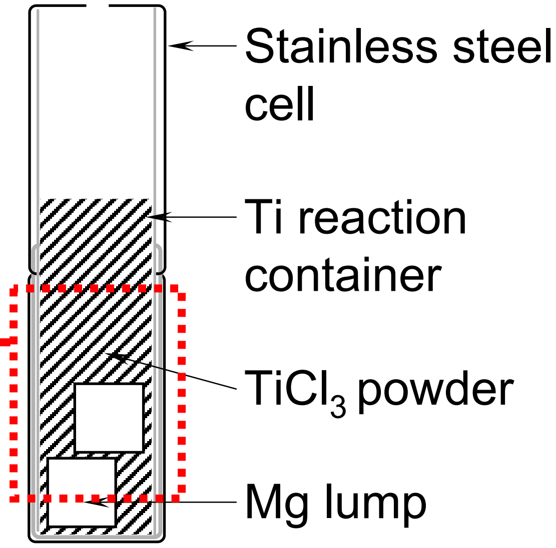

(c) Sectioned reaction container after reduction

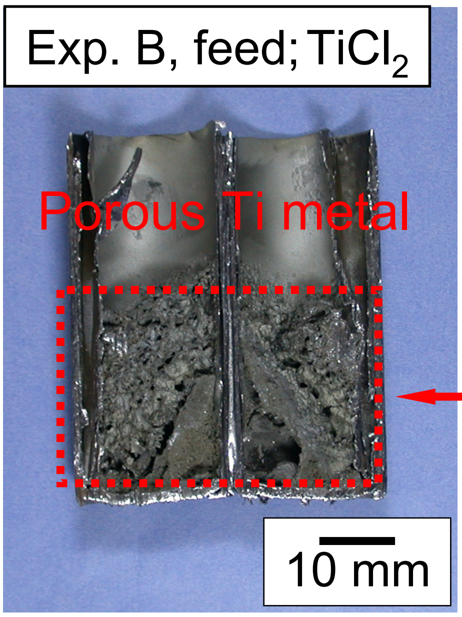

(d) Initial setup of (c)

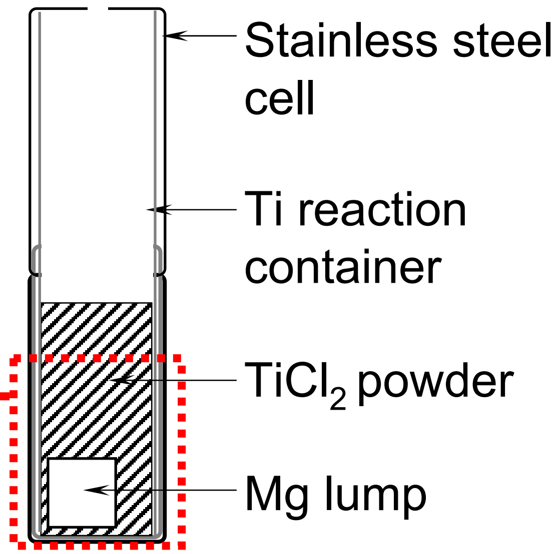

Figure Sectioned titanium reaction container after the experiment for the magnesiothermic reduction of $TiCl_x$. [G,S]

Results: XRD and Composition

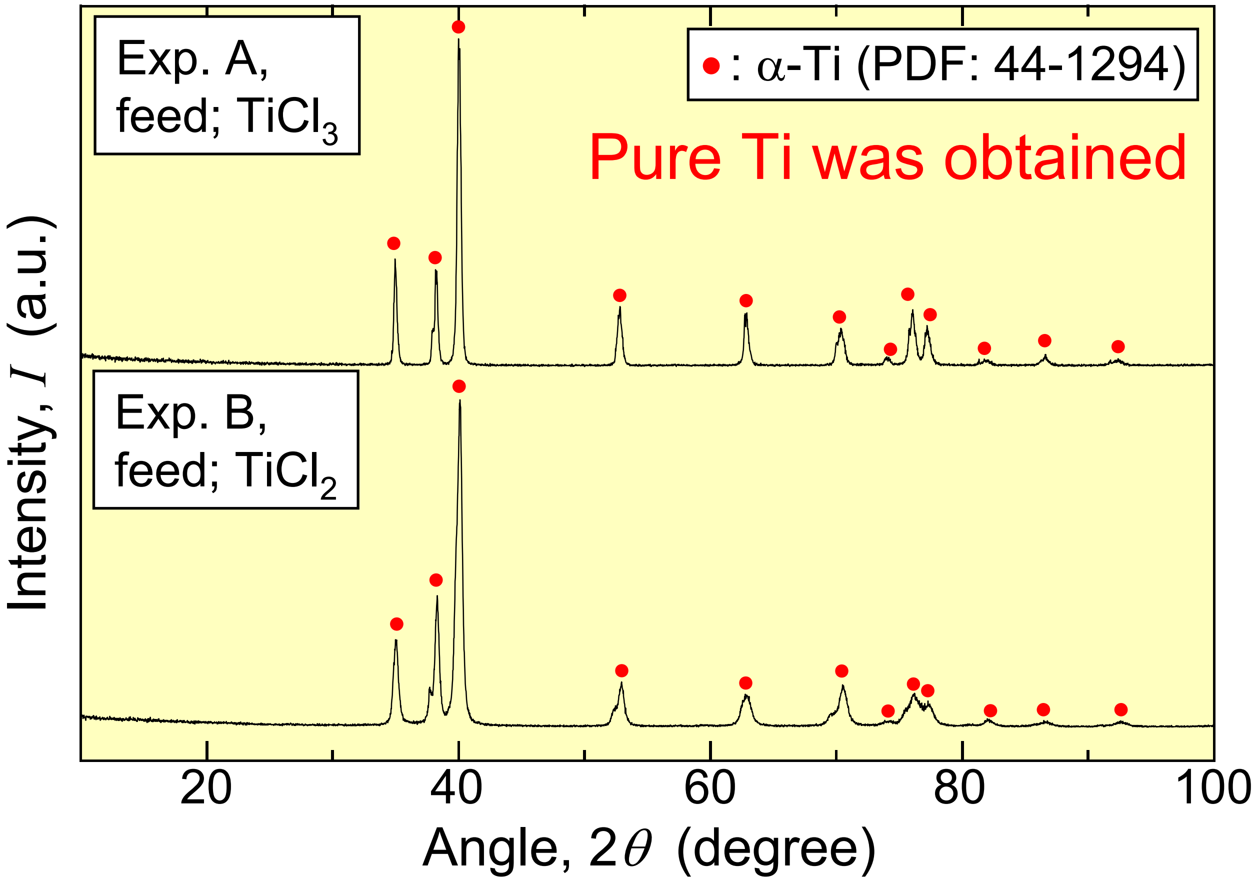

Figure X-ray diffraction patterns of the obtained powder samples. [G, R]

Table Analytical results of the obtained titanium samples

Exp.	Concentration of element i, C_i (mass%) [a]						Yield (%)
	Ti	Fe	Ni	Cr	Mg	Al	
A	99.37	0.16	<0.01	0.02	0.16	0.44	99
B	99.92	0.03	<0.01	0.04	<0.01	<0.01	94

[a] Determined by X-ray fluorescence analysis, and the value excludes carbon and gaseous elements.

[G, R]

Results: Microstructure

(a) Obtained titanium from $TiCl_3$

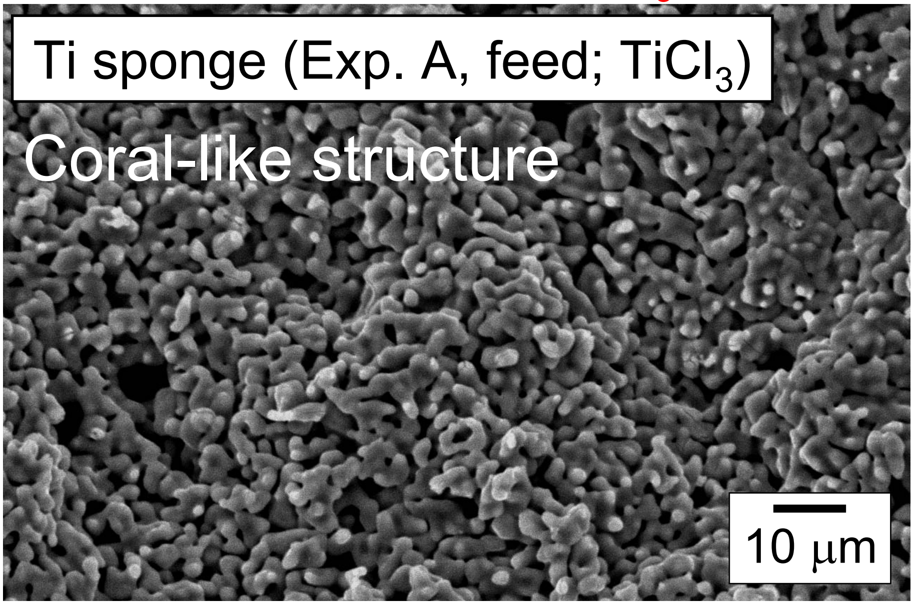

(b) Obtained titanium from $TiCl_2$

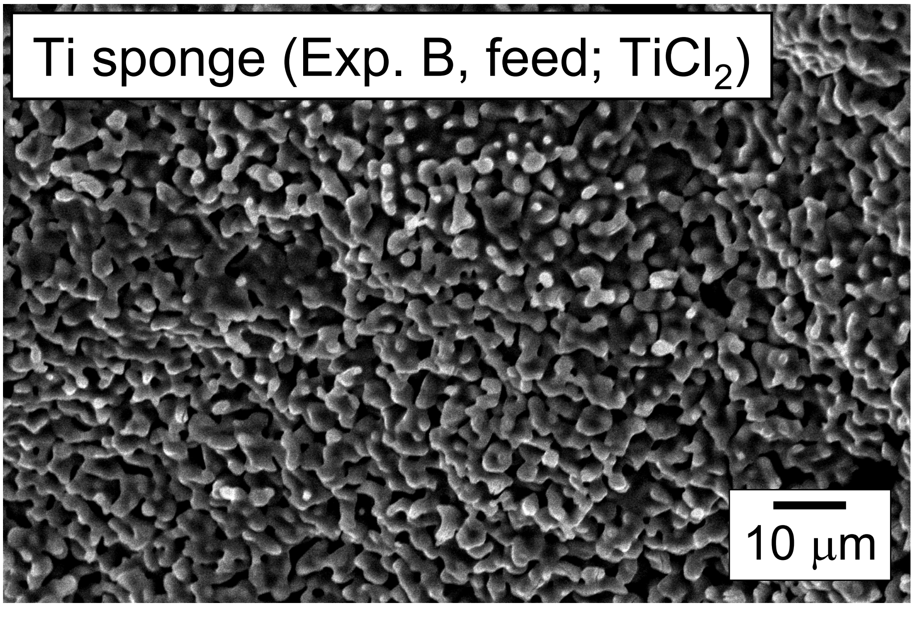

Figure Scanning electron micrographs of the obtained titanium samples. [F, Q]

Separation Process by the Combination of Draining and Vacuum Distillation

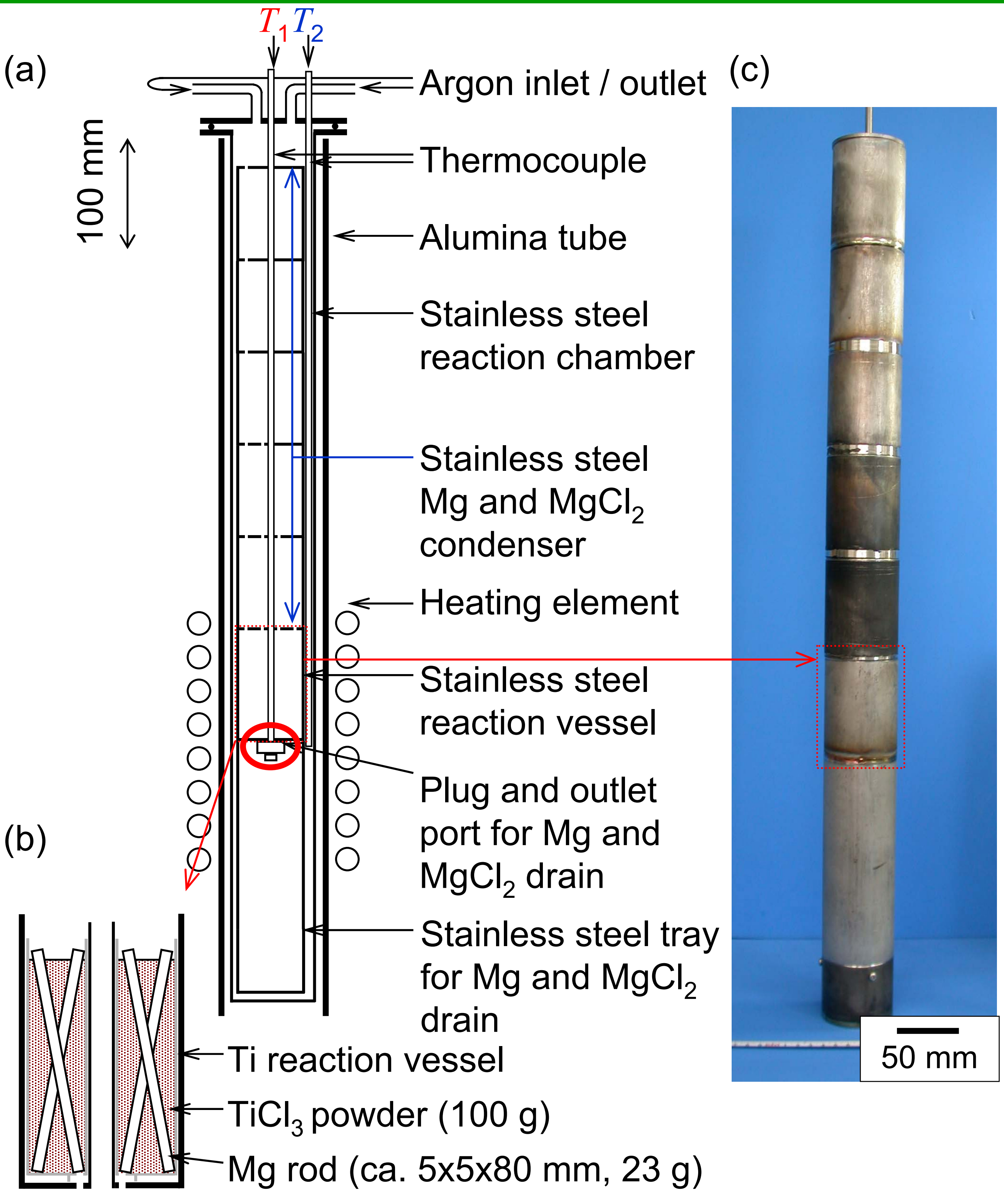

Figure Schematic illustration of the experimental apparatus for the magnesiothermic reduction of $TiCl_3$. [J]

Separation Process by the Combination of Draining and Vacuum Distillation

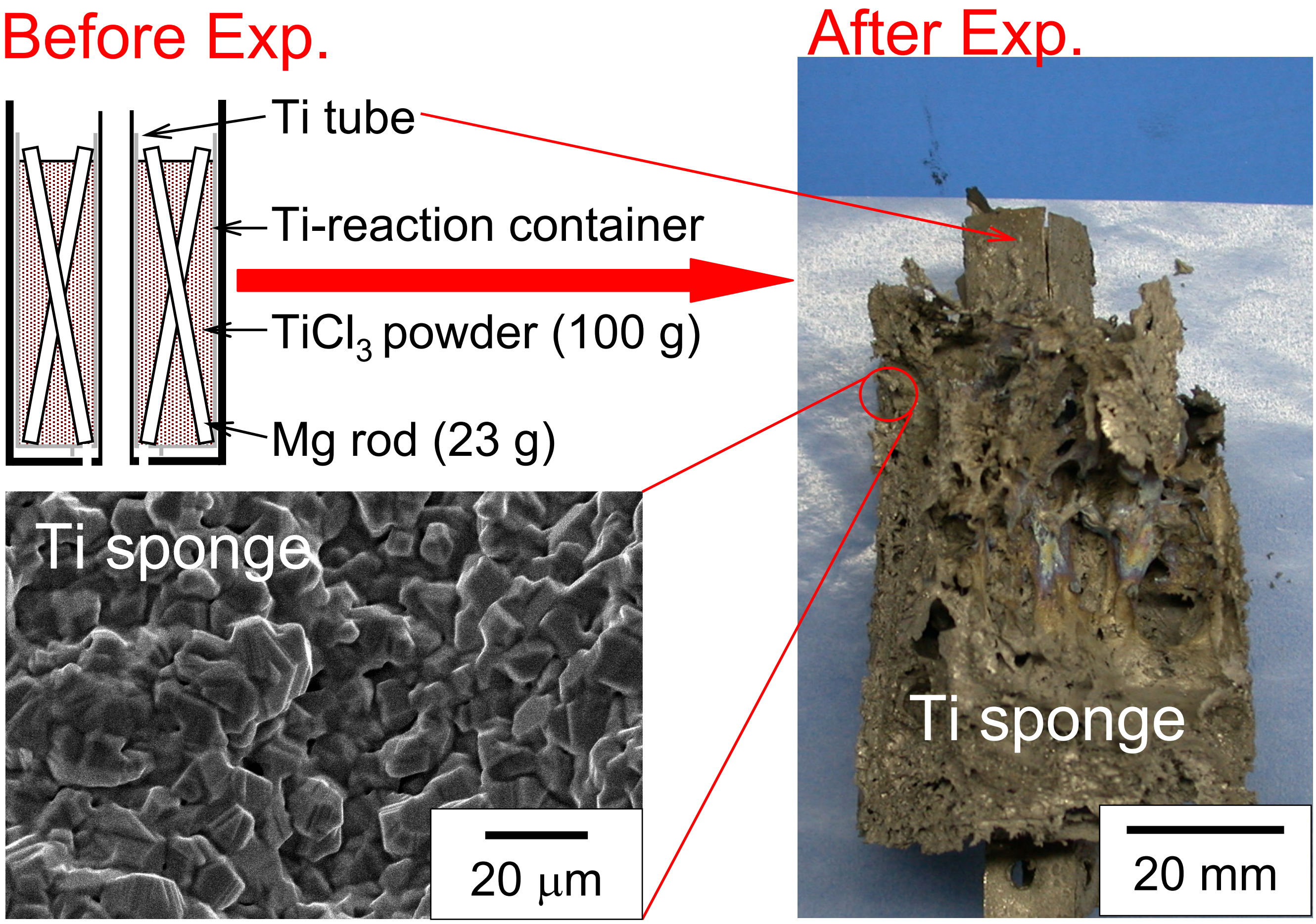

Table
Analytical results for the magnesiothermic reduction of $TiCl_3$

Exp.	Concentration of element i, C_i (mass%) [a, b]						Yield
	Ti	Fe	Ni	Cr	Mg	Al	(%)
J	99.18	0.50	0.01	0.02	0.09	0.21	87
N	99.04	0.18	0.02	0.02	0.09	0.65	82

[a] Determined by X-ray fluorescence analysis, and the obtained value excludes carbon and gaseous elements.
[b] This value is the average of top and bottom of the obtained Ti sponge.

Pure metallic titanium was effectively obtained by this process.

Conclusions

A new titanium production process based on the magnesiothermic reduction of titanium subhalides was proposed, and its feasibility was demonstrated.

Further details:

- High-speed magnesiothermic reduction of $TiCl_x$ was carried out and feasibility of this high-speed reduction process was demonstrated.

- It was demonstrated that a titanium crucible can be utilized as a construction material for the reduction process, and a new Fe-contamination free process was proposed.

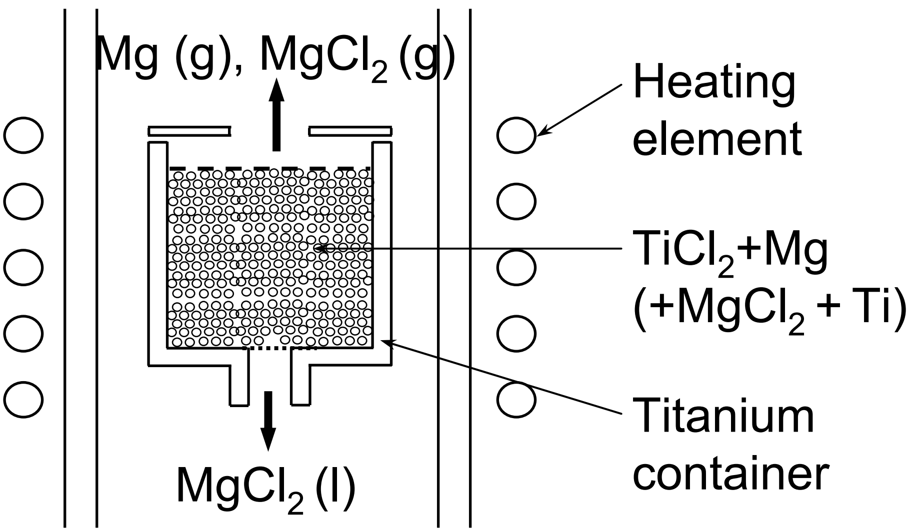

Future Works

- Production process of $TiCl_x$ from $TiCl_4$
- Enrichment process of $TiCl_x$

→ Establishment of a continuous and high-speed titanium production process

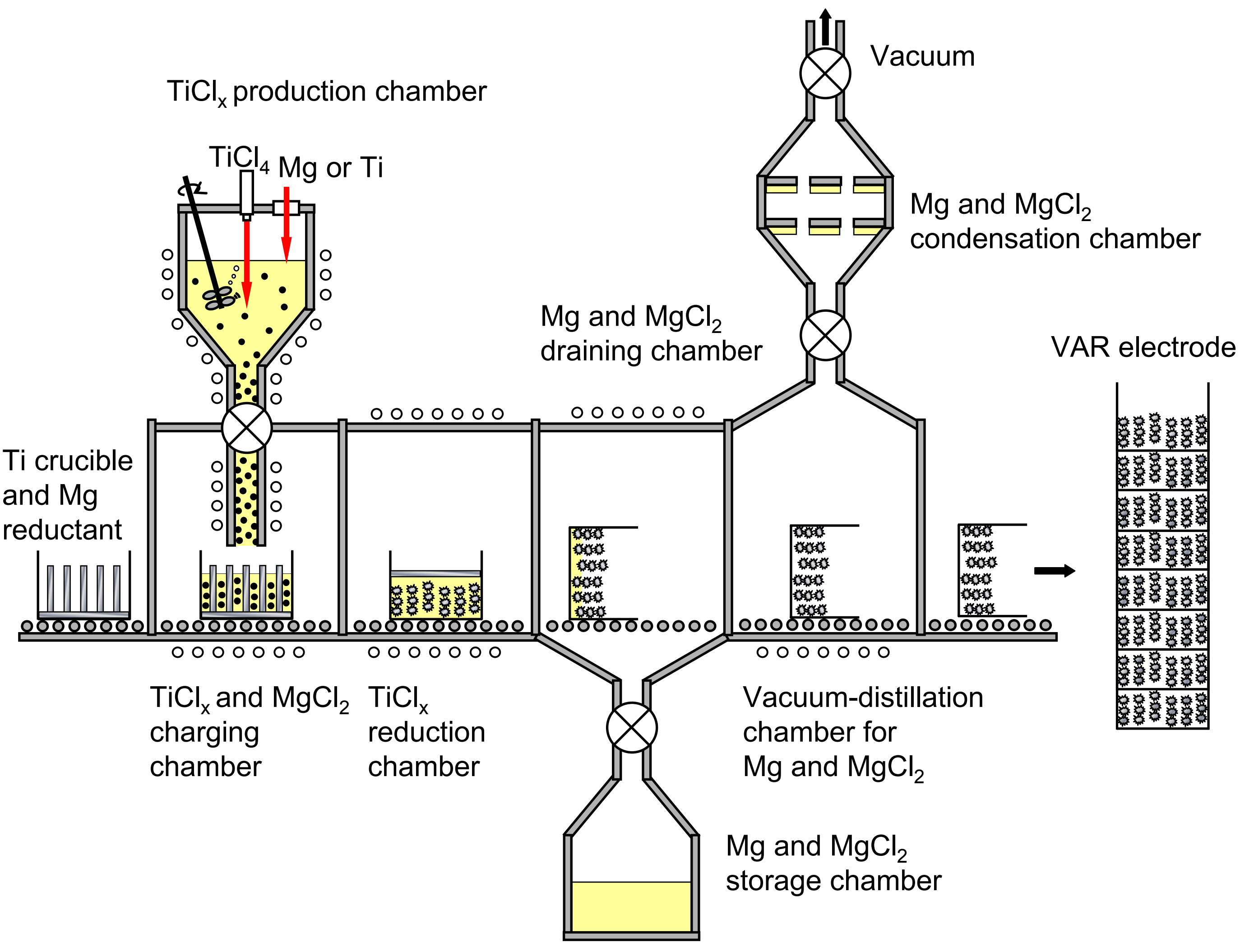

これ以後補足資料

Gibbs Energy of Formation of Chloride

$$\Delta G_f^\circ = \Delta H_f^\circ + T\Delta S_f^\circ$$

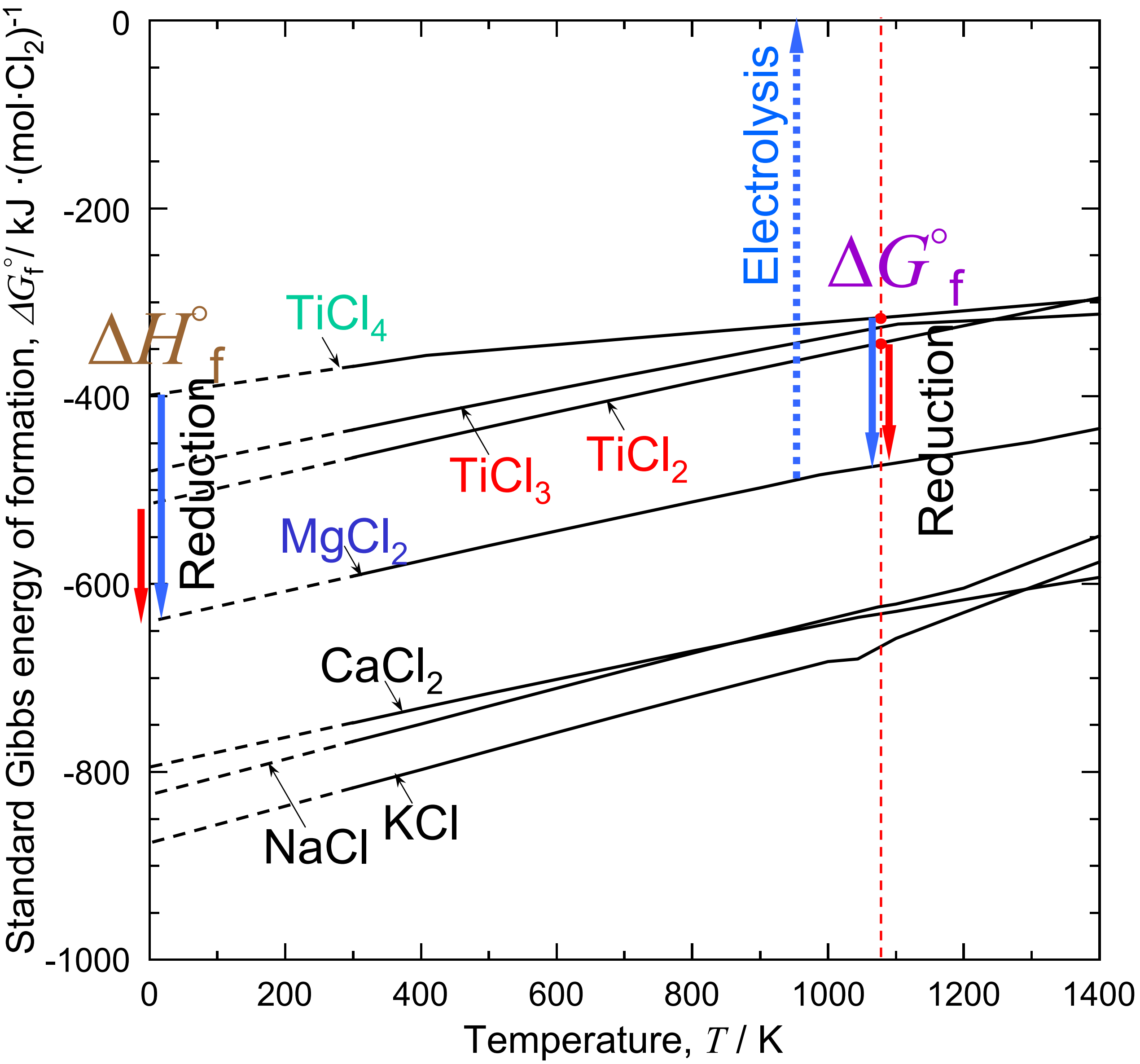

Heat of reduction is halved by utilizing titanium subhalides

Fig. Standard Gibbs energy of formation of several Chlorides.[Ref. I. Barin, Thermochemical Data of Pure Substances, VCH Verlagsgesellschaft, Weinheim, (1989).]

Elementary Reaction Equation and Total Reaction Equation

At 1073 K

① $TiCl_4(g) + Mg(l) \rightarrow TiCl_2(s) + MgCl_2(l)$

$\Delta H^\circ = -339$ kJ, $\Delta G^\circ = -185$kJ

This is suitable for developing high speed process

② $TiCl_2(s) + Mg(l) \rightarrow Ti(s) + MgCl_2(l)$

$\Delta H^\circ = -91$ kJ, $\Delta G^\circ = -130$ kJ

---

③ $TiCl_4(g) + 2\ Mg(l) \rightarrow Ti(s) + 2\ MgCl_2(l)$

(=①+②) $\Delta H^\circ = -430$ kJ, $\Delta G^\circ = -315$ kJ

Mass Balance of Titanium Production

$TiCl_4$	+	2 Mg	→	Ti	+	2 $MgCl_2$
3.96 ton		1.02 ton		1 ton		3.98 ton
2.33 m^3		0.59 m^3		0.22 m^3		1.71 m^3

$\Delta H^\circ = -8980$ MJ (2.50 MW・h)

1/2

$TiCl_2$	+	Mg	→	Ti	+	$MgCl_2$
2.48 ton		0.51 ton		1 ton		1.99 ton
0.79 m^3		0.29 m^3		0.22 m^3		0.85 m^3

$\Delta H^\circ = -1900$ MJ (0.53 MW・h)

Vapor Pressure of some Chemicals

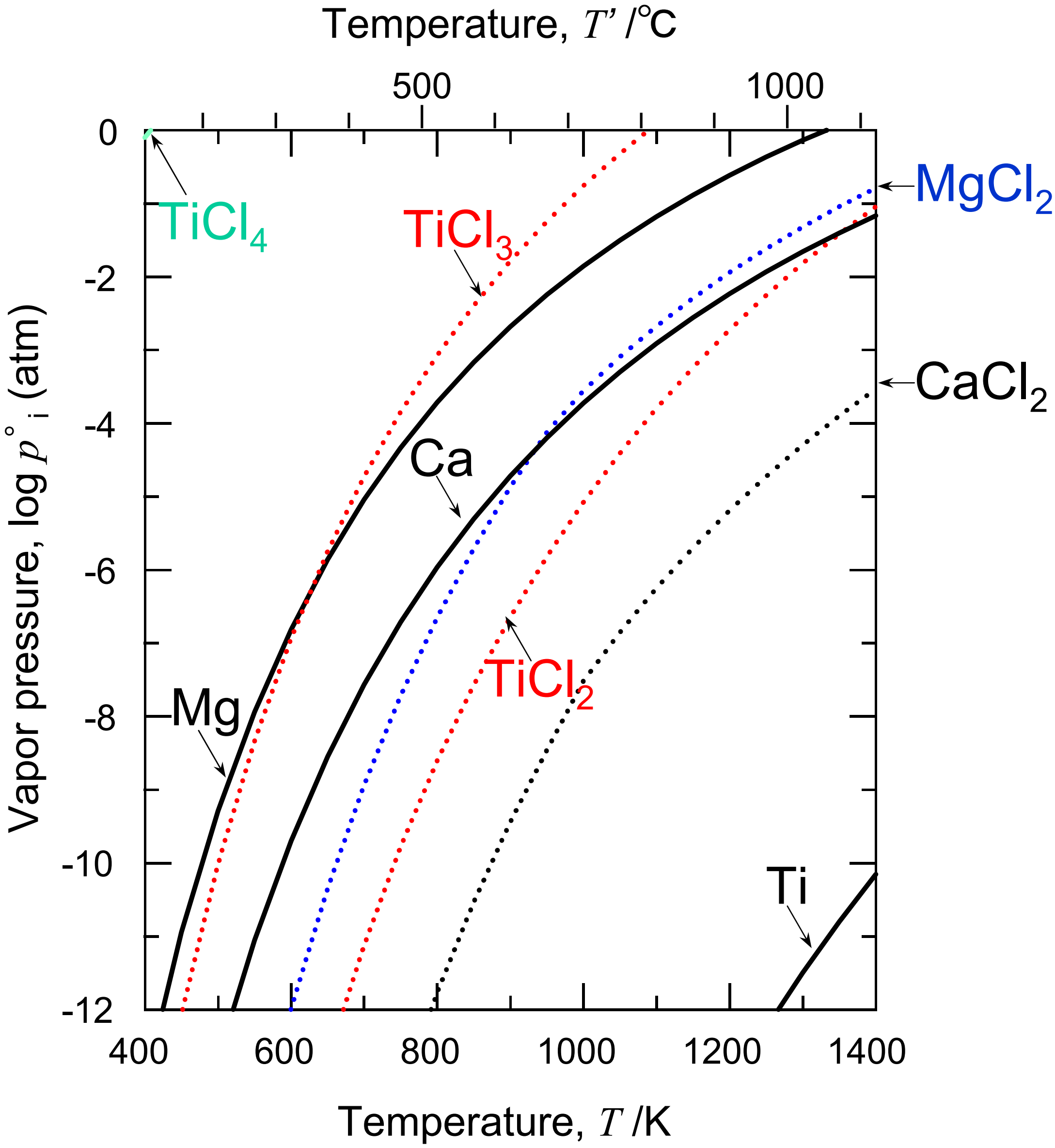

Titanium subhalides are stable as a condensed phase even at elevated temperatures

Figure Vapor pressure of several chemical species.
[Ref. I. Barin, Thermochemical Data of Pure Substances, VCH Verlagsgesellschaft, Weinheim, (1989).]

Vapor Pressure of some Chemicals

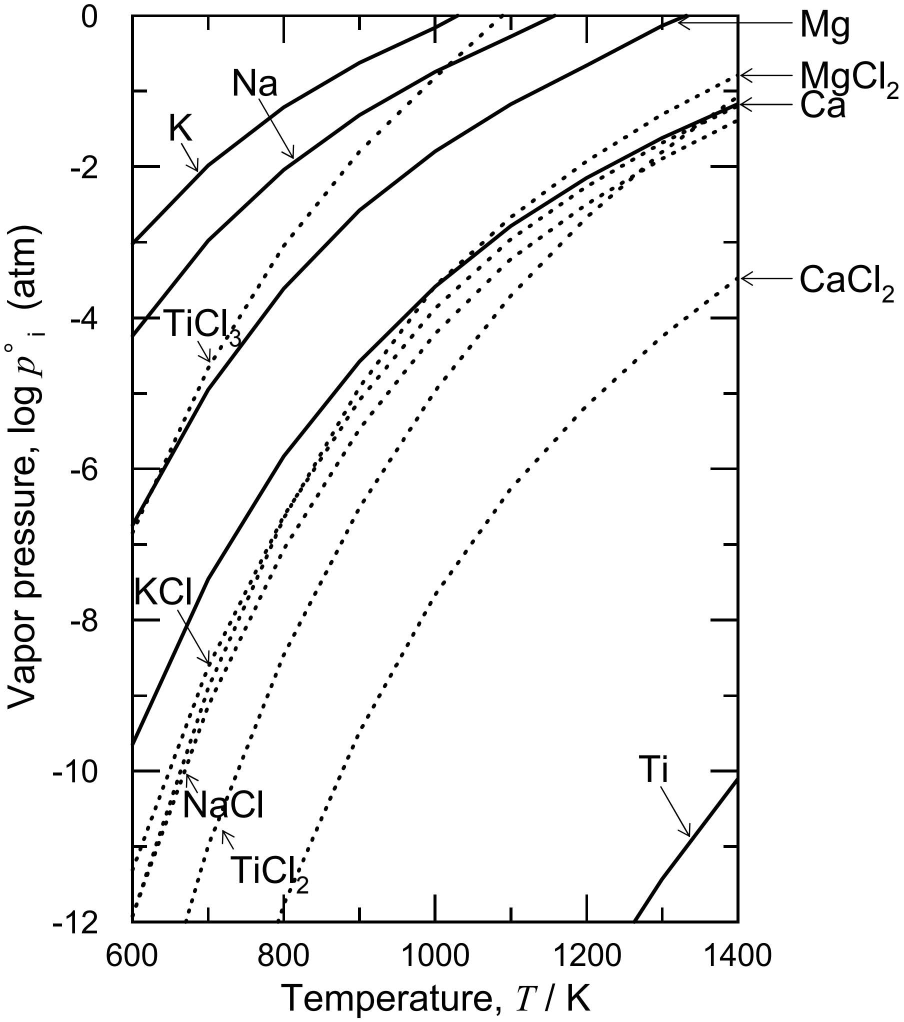

Fig. Vapor pressure of several chemical species.
[Ref. I. Barin, Thermochemical Data of Pure Substances, VCH Verlagsgesellschaft, Weinheim, (1989).]

Vapor Pressure of some Chemicals

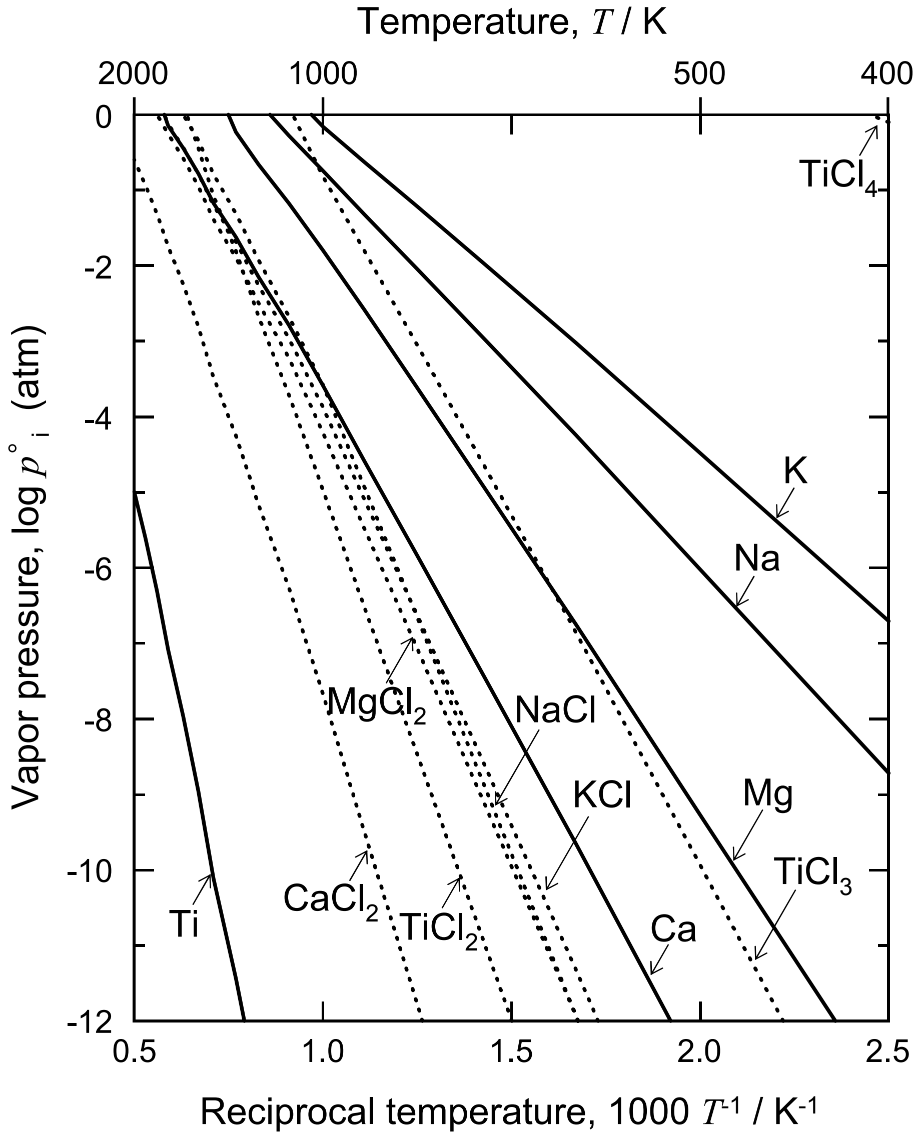

Fig. Vapor pressure of several chemical species.
[Ref. I. Barin, Thermochemical Data of Pure Substances,
VCH Verlagsgesellschaft, Weinheim, (1989).]

The Kroll Process

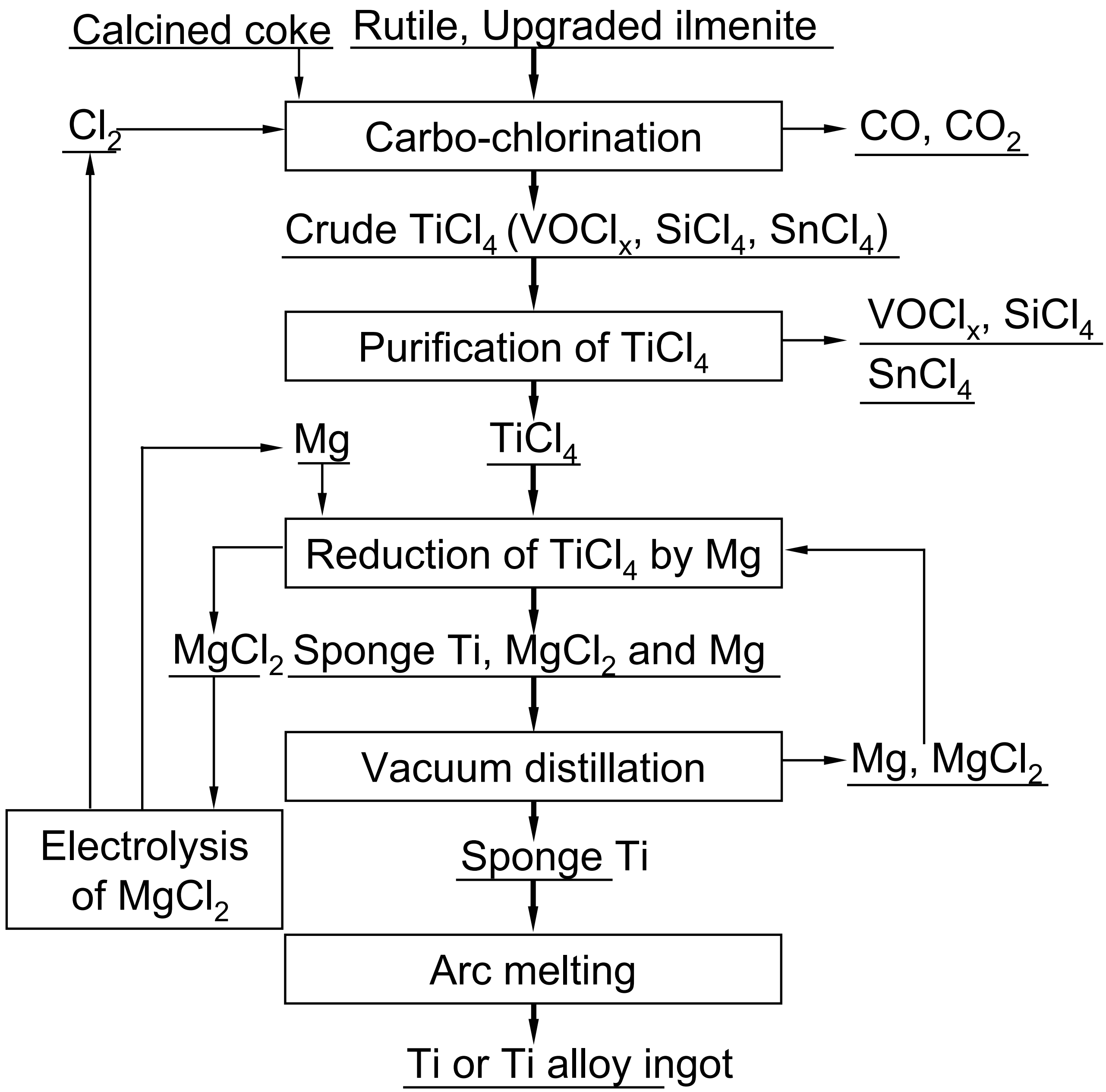

Fig Flowchart of the Kroll process for titanium production.

New Titanium Production Process Using Titanium Subhalides

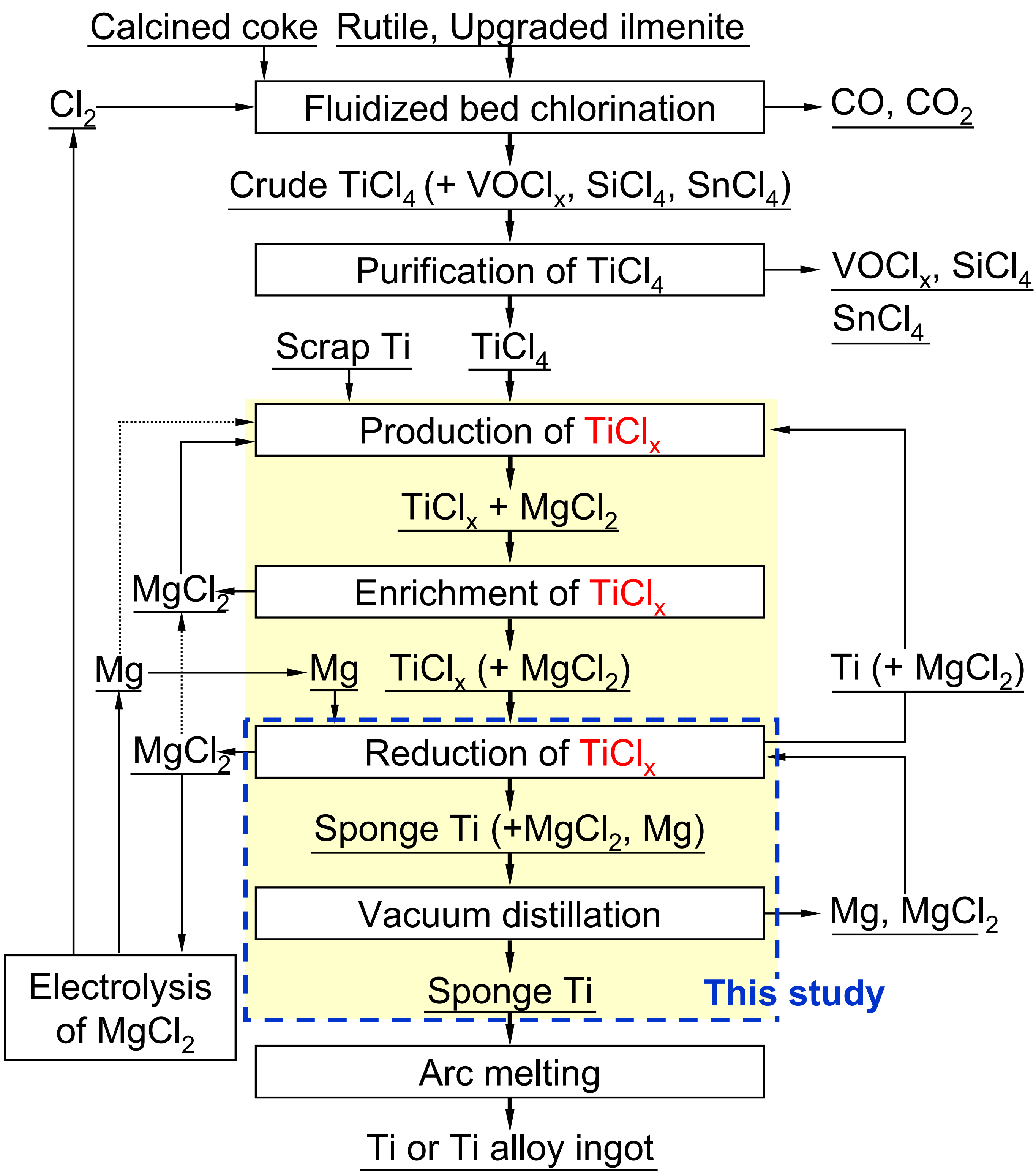

Fig Flowchart of the new titanium production process.

Key Factors of the Development of a New Titanium Reduction Process

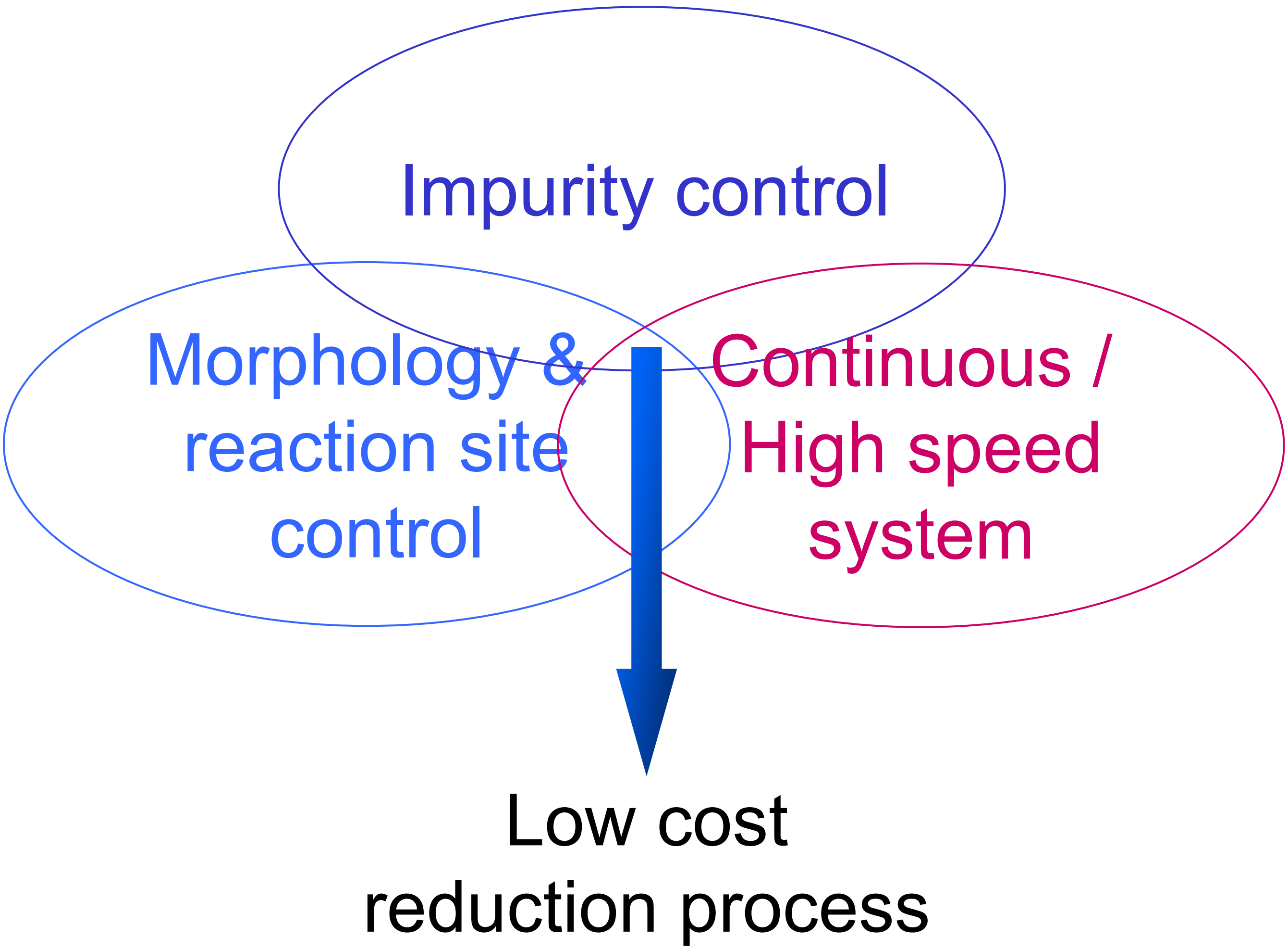

History of titanium metallurgy

1791 **Gregor**: Discovery of titanium element

1795 **Klaproth**: Denominated as "Titanium"

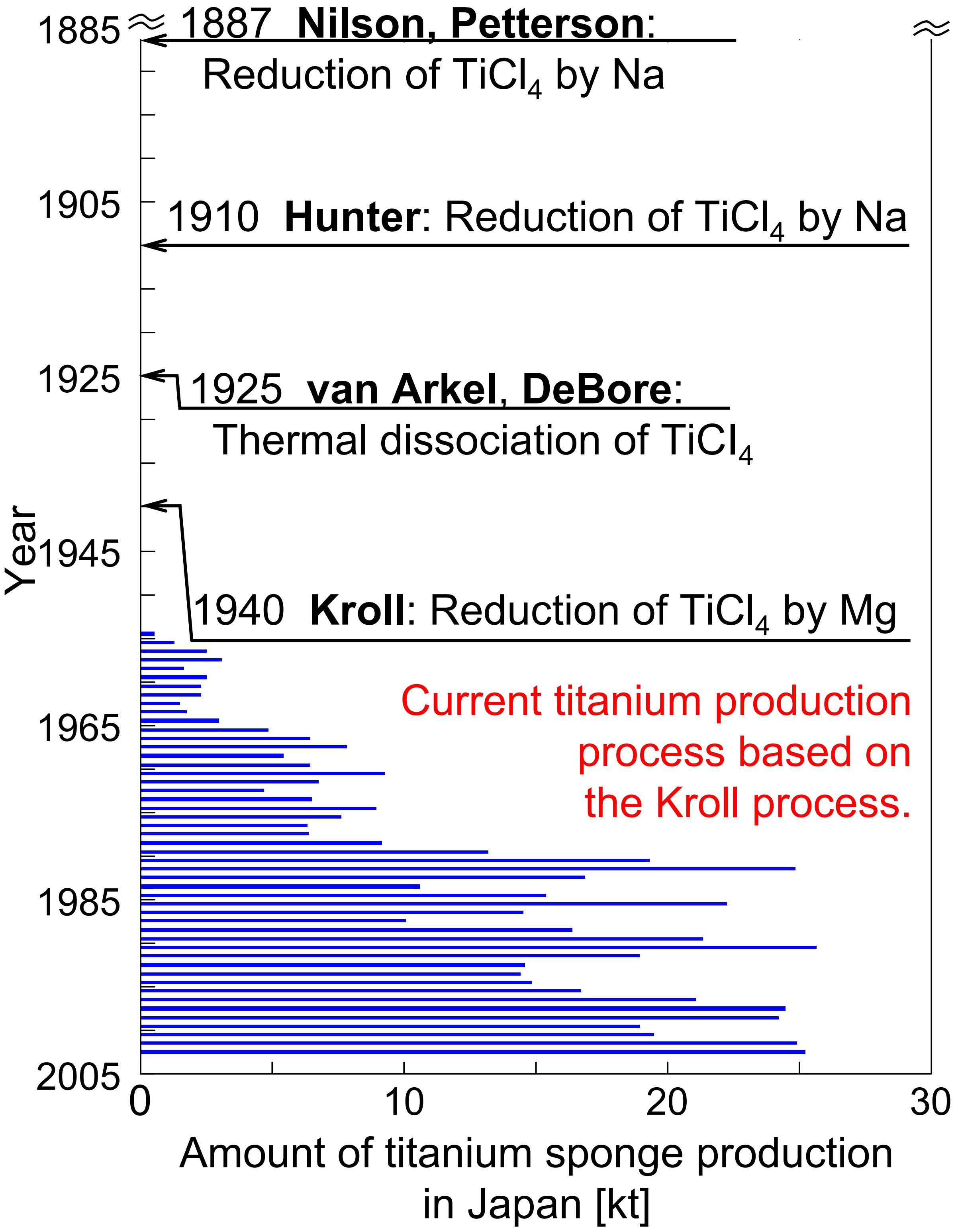

Features of the New Process

Table
Features of various reduction processes

	Advantages	Disadvantages
Kroll	◎High purity titanium available ◎Easy metal / salt separation ○Established chlorine circulation ○Utilizes efficient Mg electrolysis ○Reduction and electrolysis operation can be carried out Independently	×Complicated process ×Slow production speed ×Batch type process
FFC	◎Simple process ○Semi-continuous process	×Difficult metal / salt separation ×Reduction and electrolysis have to be carried outsimultaneously △Sensitive to carbon and iron contamination △Low current efficiency
OS	◎Simple process ○Semi-continuous process	×Difficult metal / salt separation △Sensitive to carbon and iron contamination △Low current efficiency
EMR / MSE	◎Resistant to iron and carbon contamination ○Semi-continuous process ○Reduction and electrolysis operation can be carried out Independently	×Difficult metal / salt separation when oxide system ×Complicated cell structure △Complicated process
PRP	◎Effective control of purity and morphology ◎Flexible scalability ◎Resistant to contamination ○Small amount of fluxes necessary	×Difficult recovery of reductant ×Environmental burden by leaching
This study	◎High speed reduction process ○Semi-continuous process ○Titanium scrap enable ○Facilities for Kroll process can be utilized	×Difficulty of $TiCl_2$ handling △Multiple reduction process

Reaction Mechanism in The Kroll Process

1. $TiCl_4$ is dropped into a reactor.

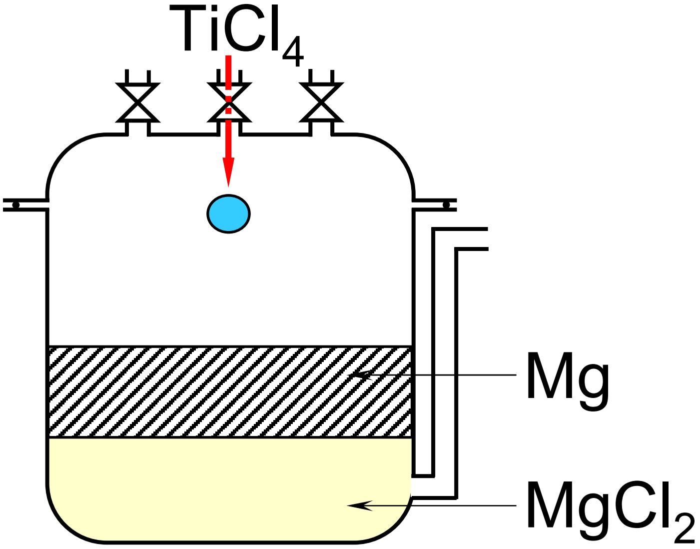

2. $TiCl_4$ vaporizes.

$$TiCl_4\ (l) \rightarrow TiCl_4\ (g)$$

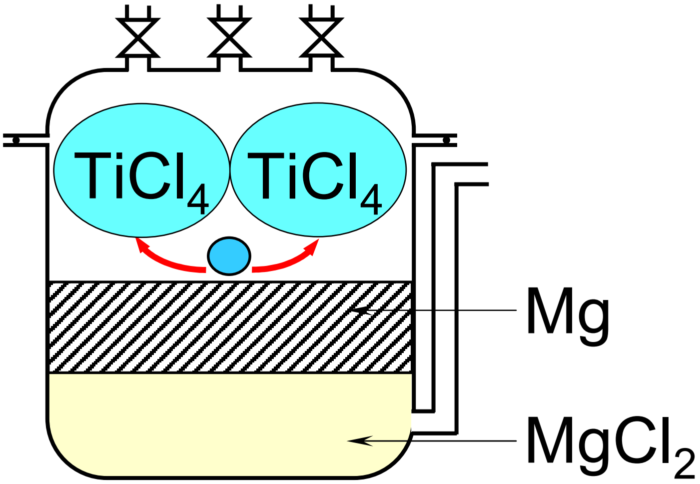

Reaction Mechanism in The Kroll Process

3. A part of gaseous $TiCl_4$ is reduced to $TiCl_2$ by Mg, and $TiCl_2$ dissolves into molten $MgCl_2$.

$$TiCl_4\ (g) + Mg\ (l) \rightarrow \underline{TiCl_2\ (l)} + MgCl_2\ (l)$$

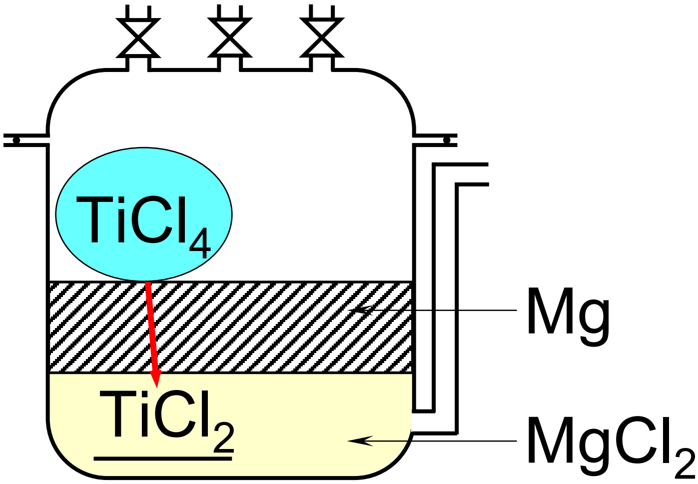

4. $TiCl_2$ is reduced to Ti by Mg.

$$\underline{TiCl_2\ (l)} + Mg\ (l) \rightarrow Ti\ (s) + MgCl_2\ (l)$$

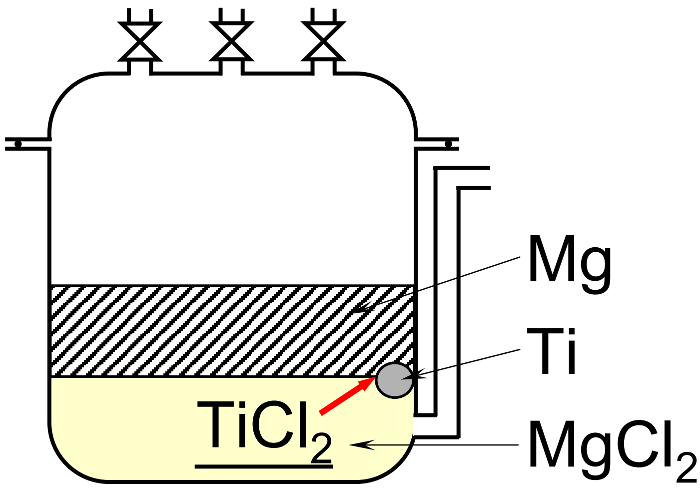

Reaction Mechanism in The Kroll Process

5. A part of gaseous $TiCl_4$ is directly reduced to Ti by Mg.

$$TiCl_4\ (g) + 2\ Mg\ (l) \rightarrow Ti\ (s) + 2\ MgCl_2\ (l)$$

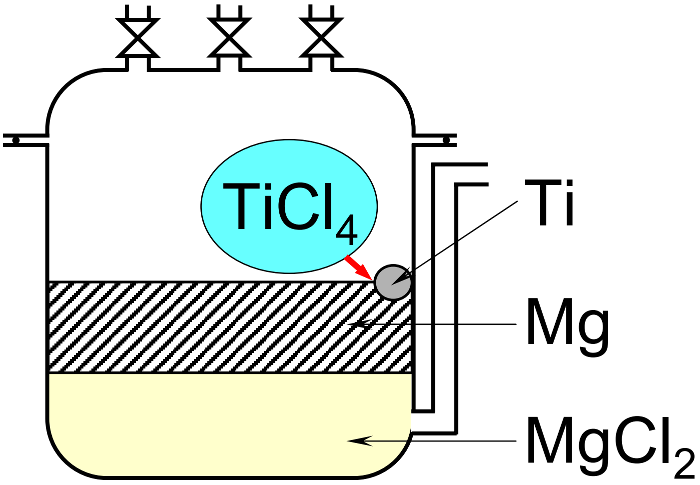

Comparison of Various Reduction Processes of Titanium Oxide in Molten Calcium Chloride Medium

(a) FFC Process (Fray *et al.*)

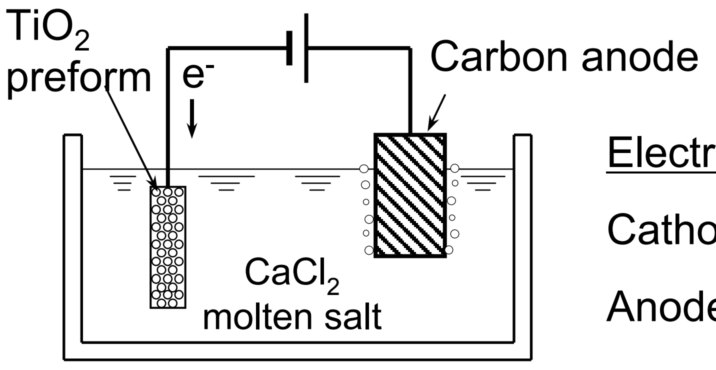

Electrolysis

Cathode: $TiO_2 + 4e^- \rightarrow Ti + 2O^{2-}$ (a1)

Anode: $C + x\,O^{2-} \rightarrow CO_x + 2x\,e^-$ (a2)

(b) OS Process (Ono & Suzuki)

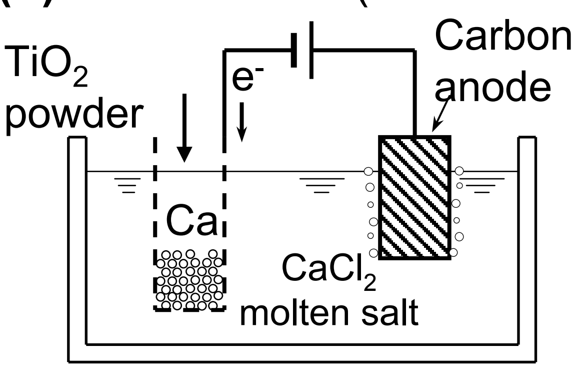

$TiO_2 + 2Ca \rightarrow Ti + 2O^{2-} + Ca^{2+}$ (b1)

Electrolysis

Cathode: $Ca^{2+} + 2e^- \rightarrow Ca$ (b2)

Anode: $C + x\,O^{2-} \rightarrow CO_x + 2x\,e^-$ (b3)

(c) EMR/MSE Process (Okabe *et al.*)

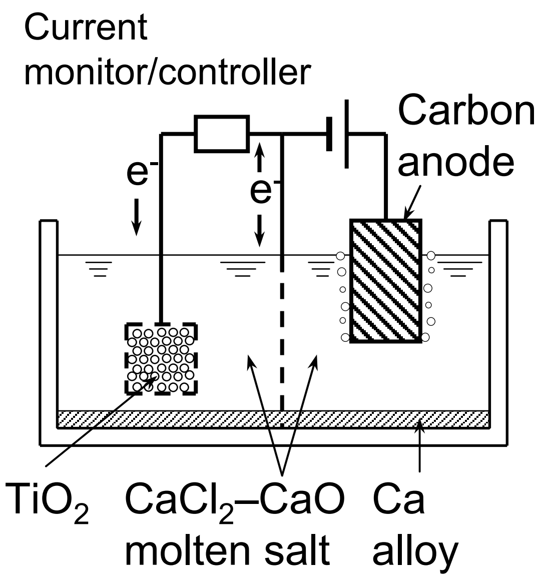

Cathode: $TiO_2 + 4e^- \rightarrow Ti + 2O^{2-}$ (c1)

Anode: $2Ca \rightarrow 2Ca^{2+} + 4e^-$ (c2)

Electrolysis

Cathode: $Ca^{2+} + 2e^- \rightarrow Ca$ (c3)

Anode: $C + x\,O^{2-} \rightarrow CO_x + 2x\,e^-$ (c4)

Overall reaction

$TiO_2 + C \rightarrow Ti + CO_2$ (d)

Properties of Materials Used in this Study

Table Physical properties of chemical species used in this study.

Symbol of chemical species	Name of chemical species	Molecular weight	Density at 20 °C, d_{20} / g·cm^{-3}	Melting point, T_m' / °C	Melting point, T_m / K	Boiling point, T_b' / °C	Boiling point, T_b / K	Sublimation point T_s' / °C	Sublimation point T_s / K
Ti	Titanium	47.88 [a]	4.5 [a]	1680 [a] 1660 [d]	1953 [a] 1933 [d]	3262 [a] 3300 [d]	3535 [a] 3573 [d]	— [a] — [d]	— [a] — [d]
$TiCl_2$	Titanium (II) chloride	118.77 [b]	3.13 [c]	1035 [c] — [e]	1308 [c] — [e]	1500 [c] — [e]	1773 [c] — [e]	— [c] 1307 [e]	— [c] 1580 [e]
$TiCl_3$	Titanium (III) chloride	154.22 [b]	no data	— [e]	— [e]	— [e]	— [e]	830 [e]	1103 [e]
$TiCl_4$	Titanium (VI) chloride	189.67 [b]	1.702 [c]	-24.1 [c] -24.1 [e]	249.1 [c] 249.1 [e]	136.5 [c] 134.9 [e]	409.7 [c] 408 [e]	— [c] — [e]	— [c] — [e]
Mg	Magnesium	24.31 [a]	1.74 [a]	659 [a] 649 [d]	932 [a] 922 [d]	1103 [a] 1090 [d]	1376 [a] 1363 [d]	— [a] — [d]	— [a] — [d]
$MgCl_2$	Magnesium (II) chloride	95.21 [b]	2.325 [c]	714 [c] 714 [d]	987 [c] 987 [d]	1412 [c] 1410 [d]	1685 [c] 1683 [d]	— [c] — [d]	— [c] — [d]
Cl_2	Chlorine	70.90 [b]	3.21 x 10^{-3} [d]	-101 [c] -101 [d]	172 [c] 172 [d]	-34.6 [c] -34.1 [d]	238.6 [c] 239.1 [d]	— [c] — [d]	— [c] — [d]

a: *Kinzoku Data Book*, 3rd ed. , (ed. by Japan Inst. Metals, Maruzen, Tokyo, 1993) pp. 1-11.
b: Calculated from reference a.
c: M. Nakahara: *Dictionary of Inorganic Compounds & Complexes*, (Koudansya, Tokyo, 1997) p 87.
d: R. Kubo *et al*. : *Rikagaku Jiten*, 4th ed. , (Iwanami Shyoten, Tokyo, 1992) pp 159-784.
e: I. Barin: *Thermochemical Data of Pure Substances*, (VCH Verlagsgesellschaft, Weinheim, 1989)

Table Temperature at specific vapor pressure

	Temperature at vapor pressure 0.01 atm		Temperature at vapor pressure 0.1 atm	
	$T'_{p0.01}$ / °C	$T_{p0.01}$ / K	$T'_{p0.1}$ / °C	$T'_{p0.1}$ / K
$TiCl_2$	1010	1283	1133	1407
$TiCl_3$	613	887	707	980
Mg	701	975	859	1133
$MgCl_2$	922	1195	1085	1358

Properties of Materials Used in this Study

Table
Composition of titanium tri-chloride [a] used in this study

Element i	Composition of element i	
	x'_i (mass%)	x_i (mol%)
Ti	24.3	18.9
Cl	71.1	74.8
Al	4.5	6.3
$TiCl_{2.96}$	77.6 [b]	75.1 [b]
$AlCl_3$	22.4 [b]	24.9 [b]

a: Supplied by Toho titanium Co., Ltd.
b: Calculated value.

This chemical is produced as a catalyst for polymerization of polypropylene.

Enrichment of $TiCl_x$

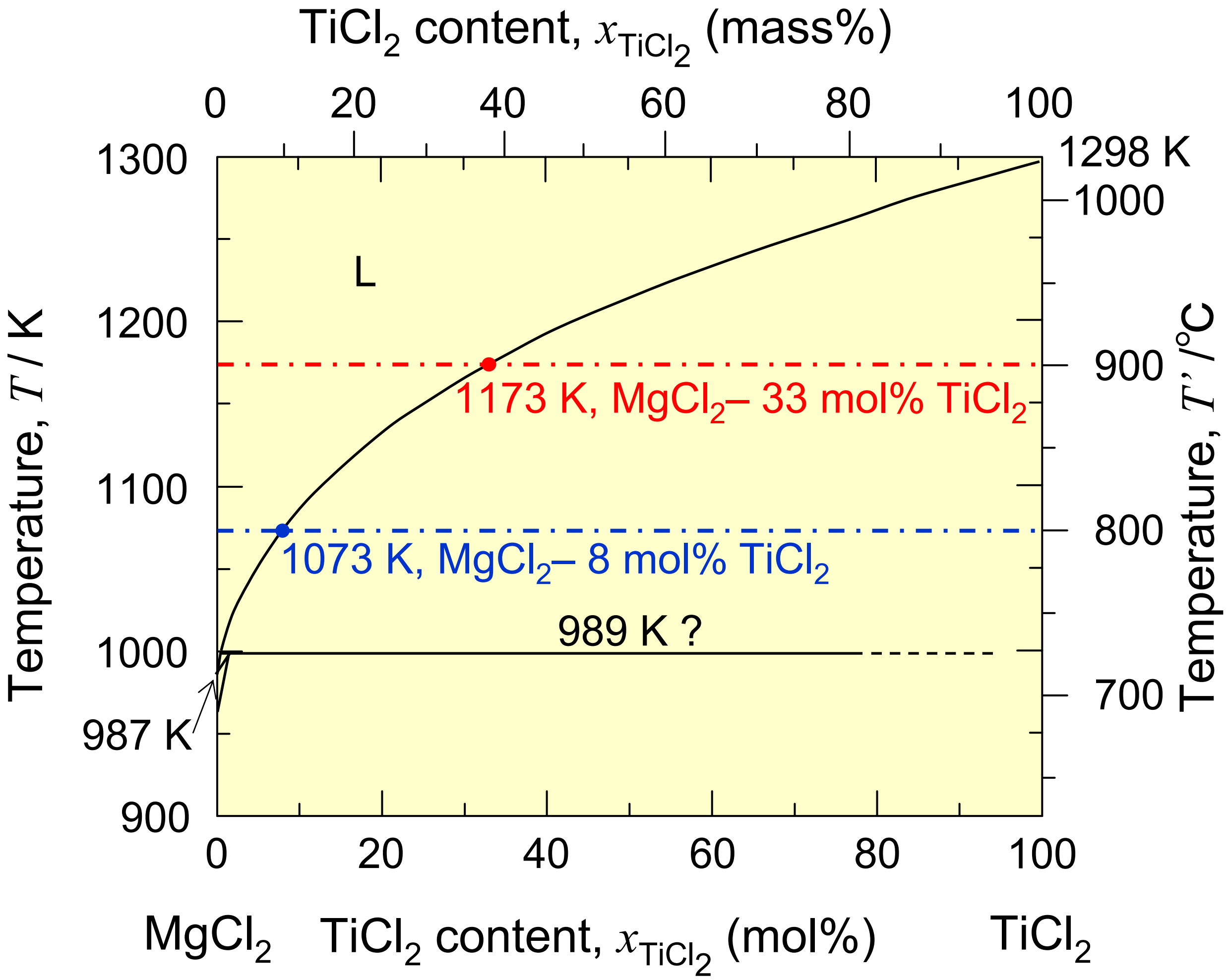

Fig. Phase diagram for the $MgCl_2$-$TiCl_2$ system.
[Ref. K. Komarek and P. Herasymenko:
J. Electrochem. Soc. 105 (1958) p 210.]

Enrichment of $TiCl_x$

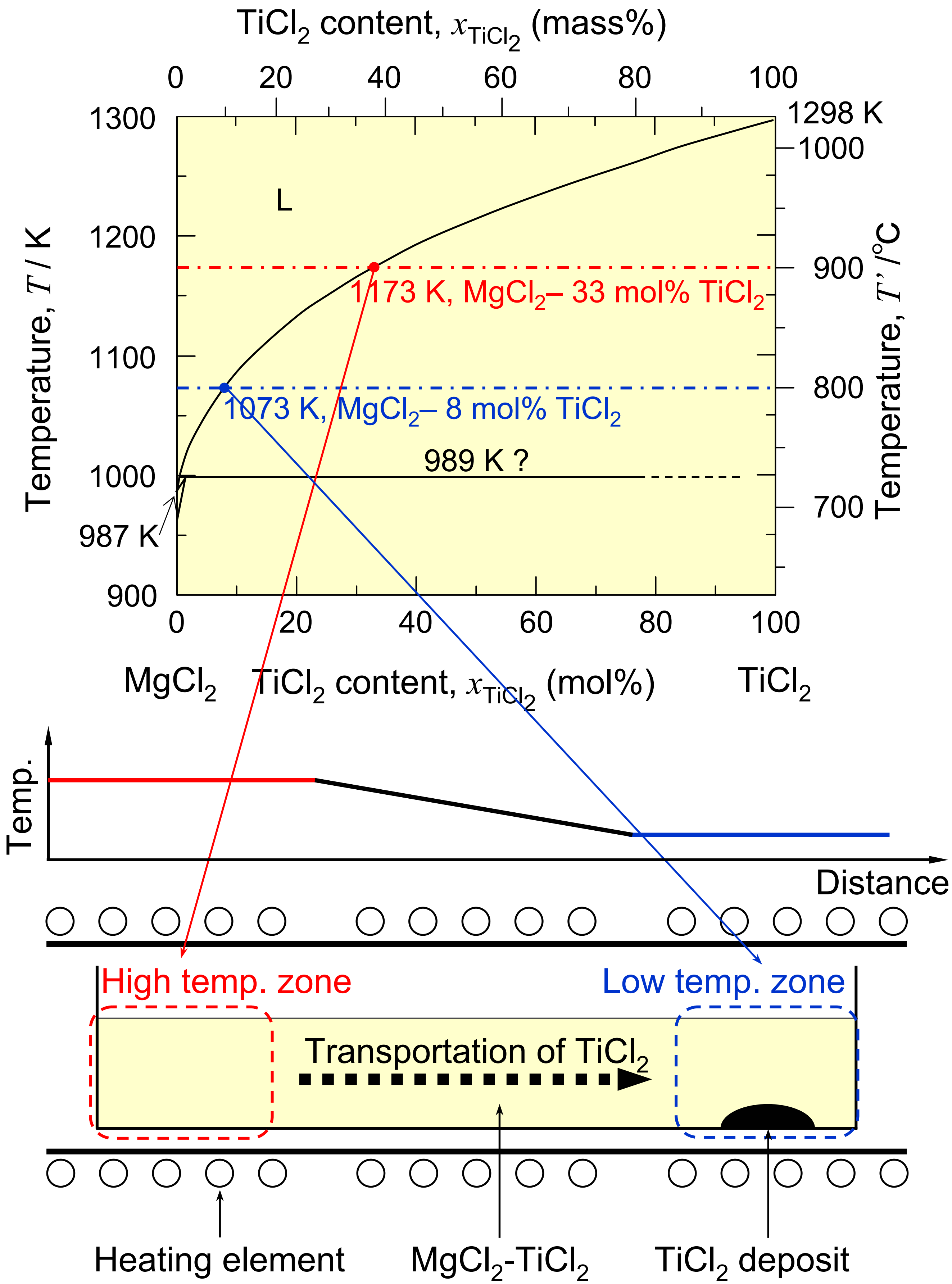

Experimental Apparatus, Small Scale, Wet/Dry Separation

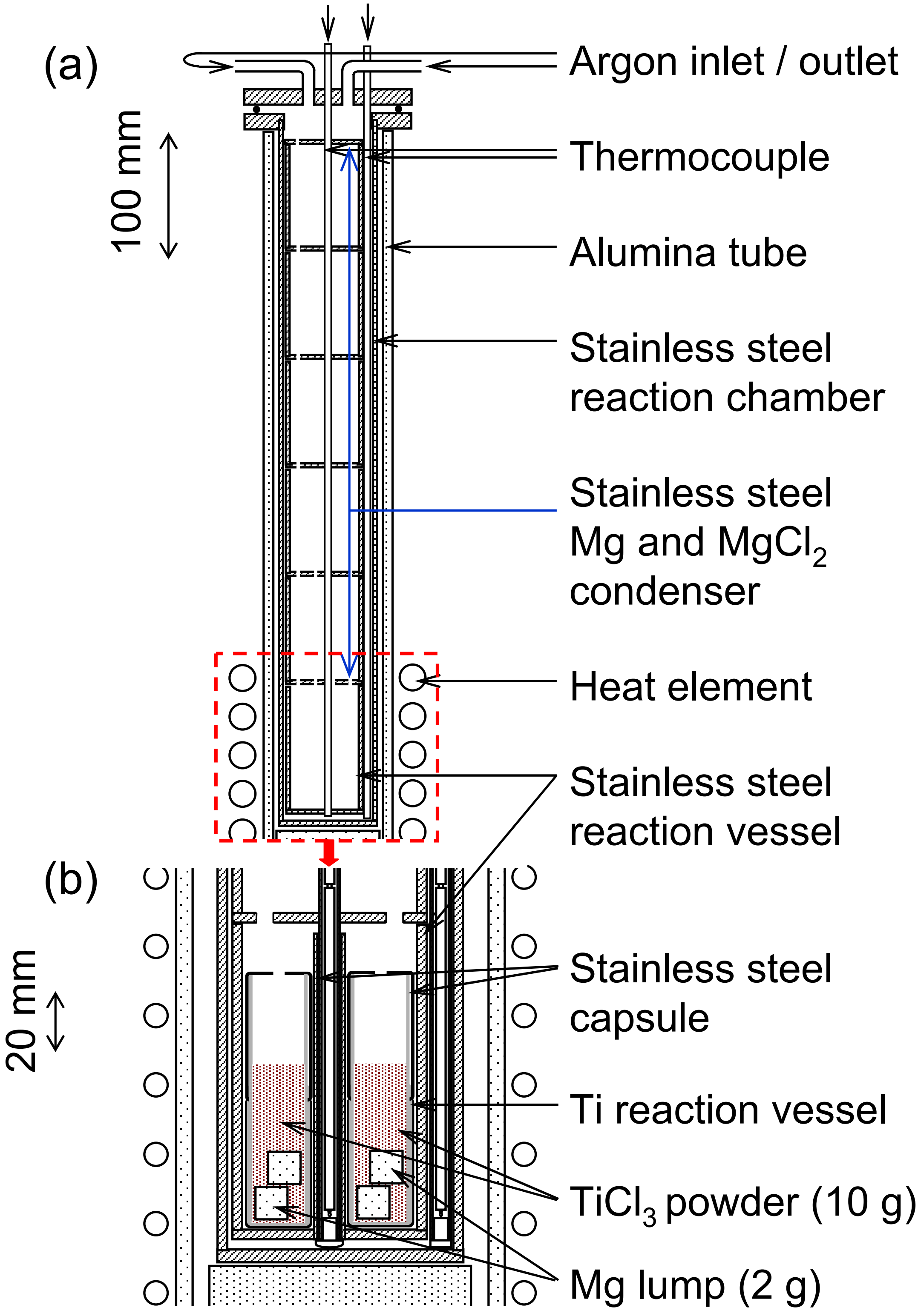

Fig. Schematic illustration of the experimental apparatus for the magnesiothermic reduction of $TiCl_3$. (Exp. o & g)
(a) Total appearance, (b) reaction vessel part.

Results, Small Scale, Wet/Dry Separation

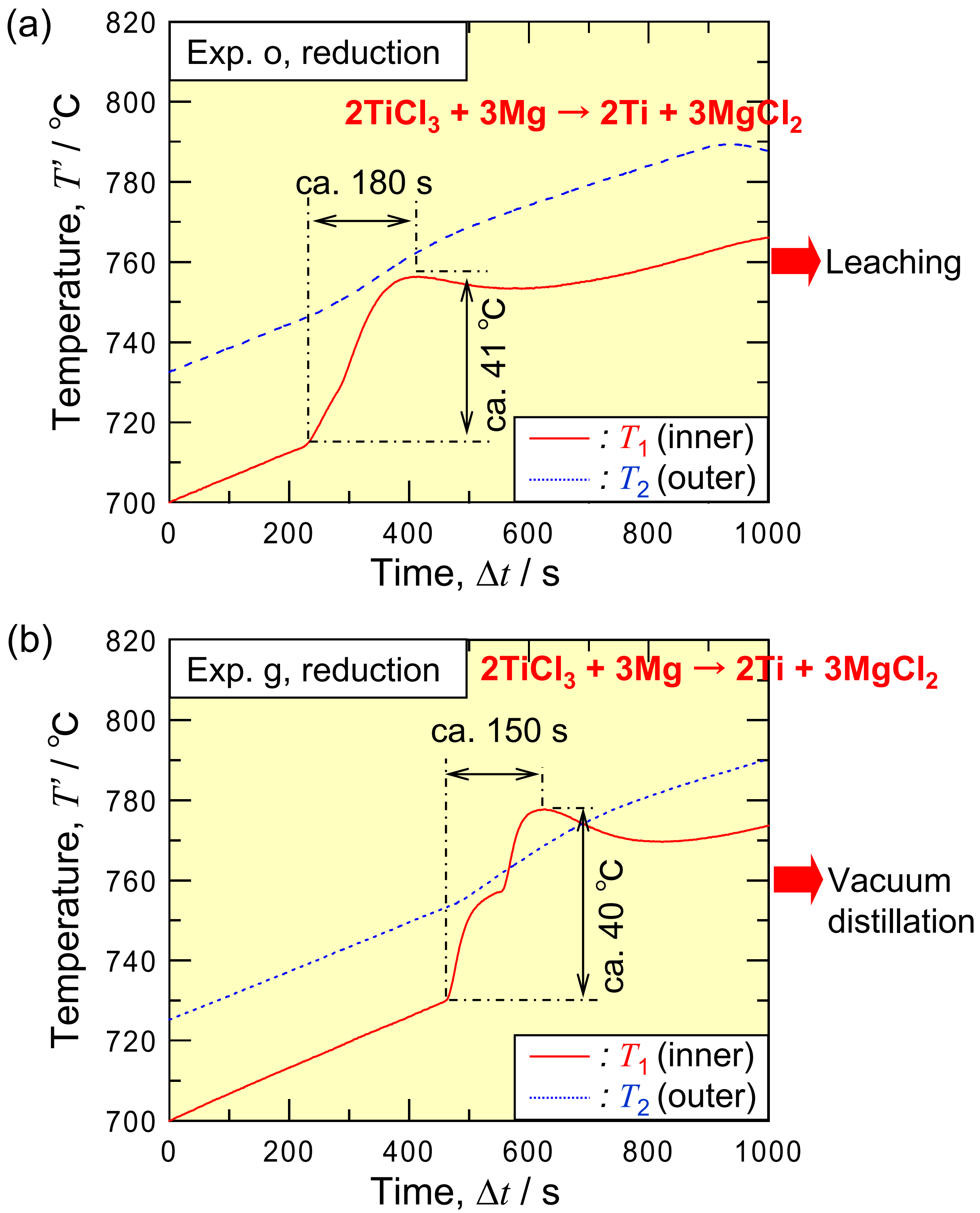

Fig. Transition of sampler temperature on the experiment of magnesiothermic reduction of $TiCl_3$, (a) Exp. o, (b) Exp. g.

Results, Small Scale, Wet/Dry Separation

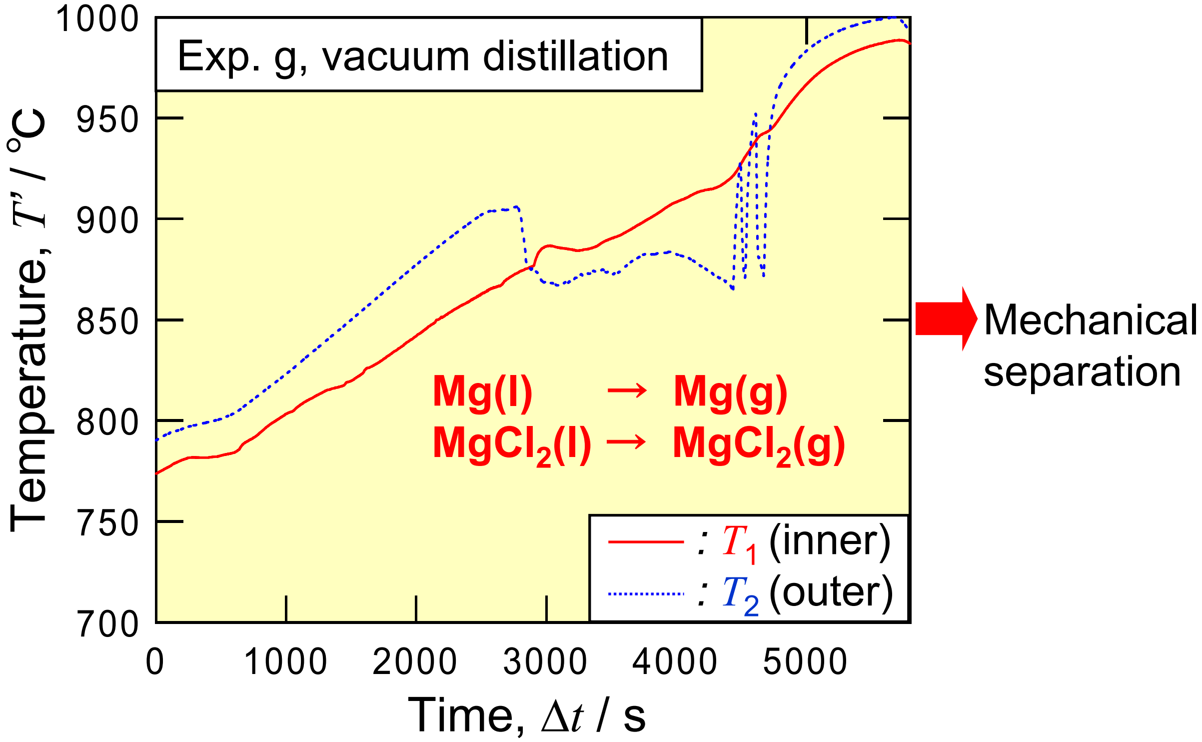

Fig. Transition of sampler temperature on the removal of Mg and $MgCl_2$ from titanium product (Exp. g).

Results, Small Scale, Wet/Dry Separation

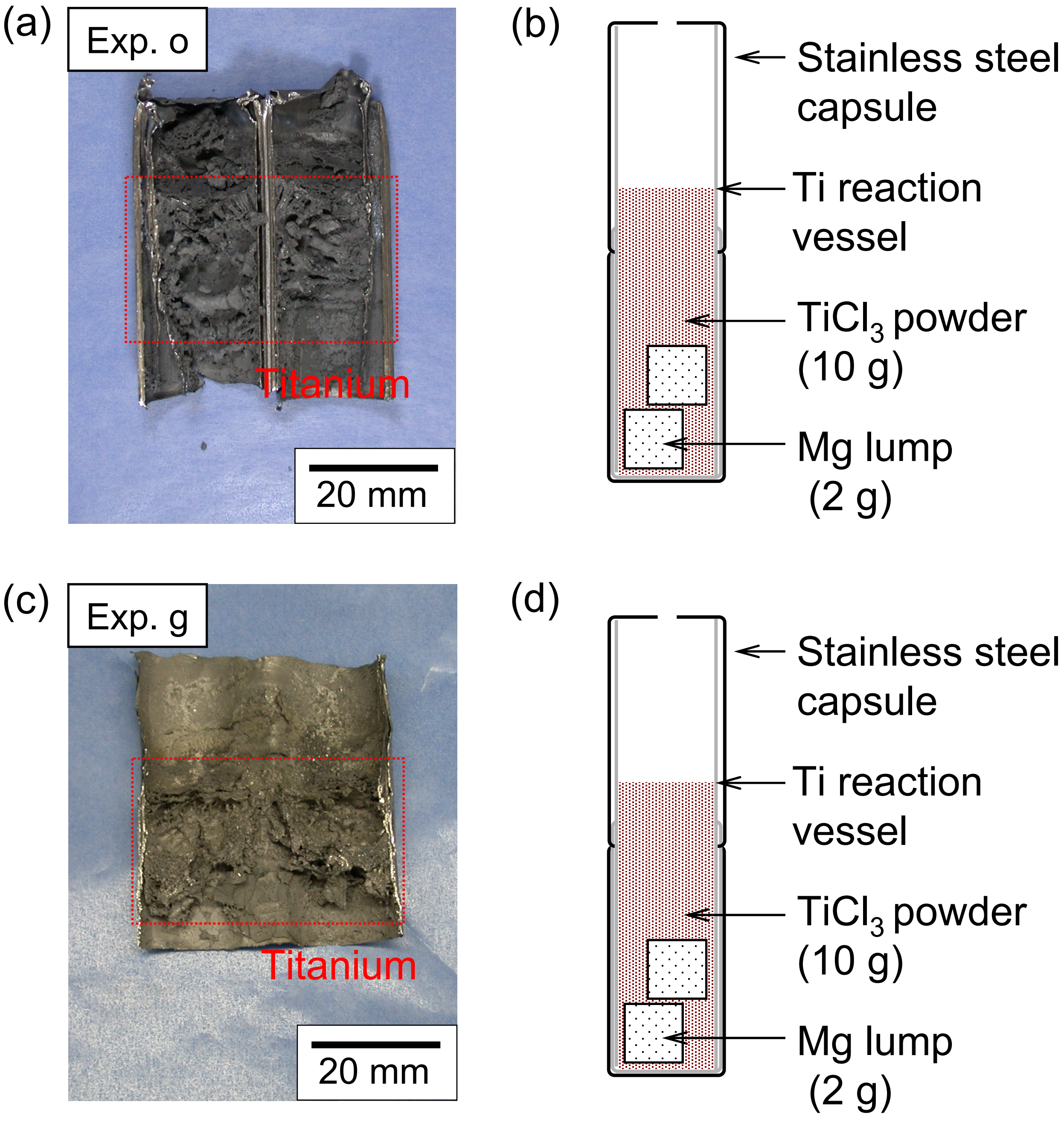

Fig. Photograph of sectioned stainless steel capsule after the experiment of magnesiothermic reduction of $TiCl_3$ and schematic illustration of initial setup before experiment, (a) (b) Exp. o, (c) (d) Exp. g.

Results, Small Scale, Wet/Dry Separation

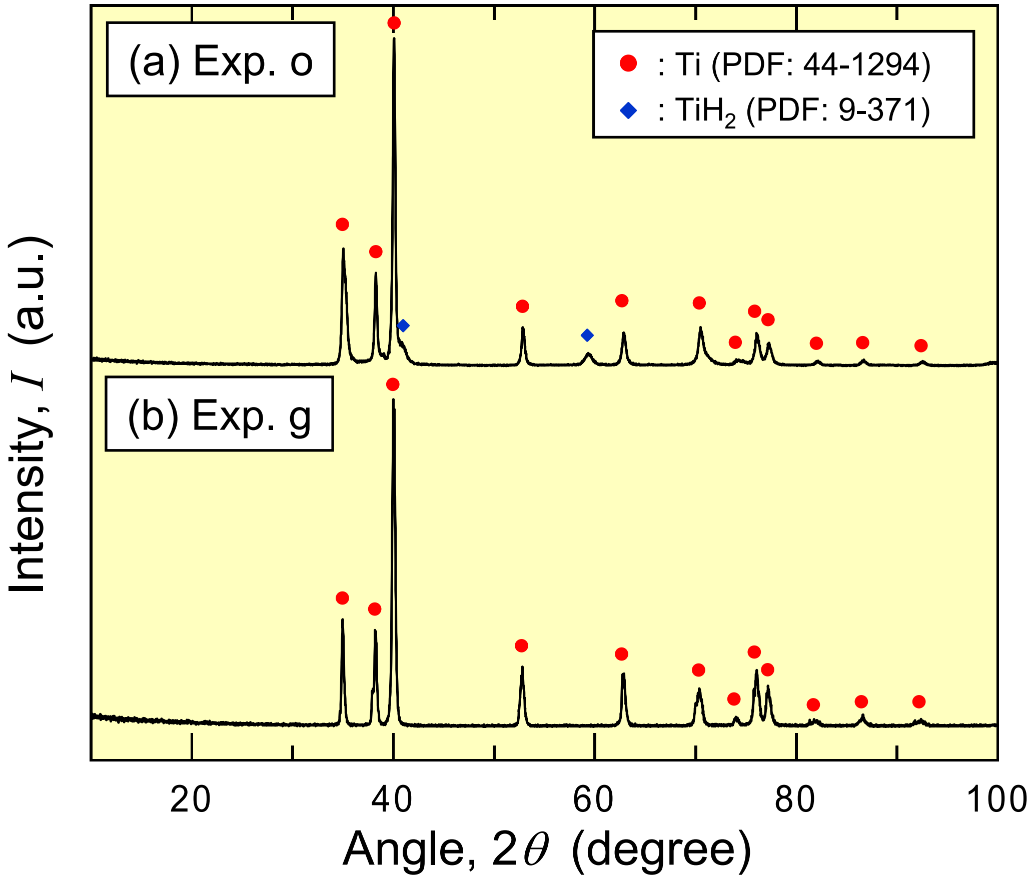

Fig. X-ray diffraction patterns of the obtained samples.

Table
Experimental results for the magnesiothermic reduction of $TiCl_3$.

Exp.	Concentration of element i, C_i (mass%) [a]						Yield
	Ti	Fe	Ni	Cr	Mg	Al	(%)
o	96.35	0.13	<0.01	0.03	0.02	3.47	86
g	99.37	0.16	<0.01	0.02	<0.01	0.44	99

[a]: Determined by X-ray fluorescence analysis, and the value exclueds carbon and gaseous elements.

Results, Small Scale, Wet/Dry Separation

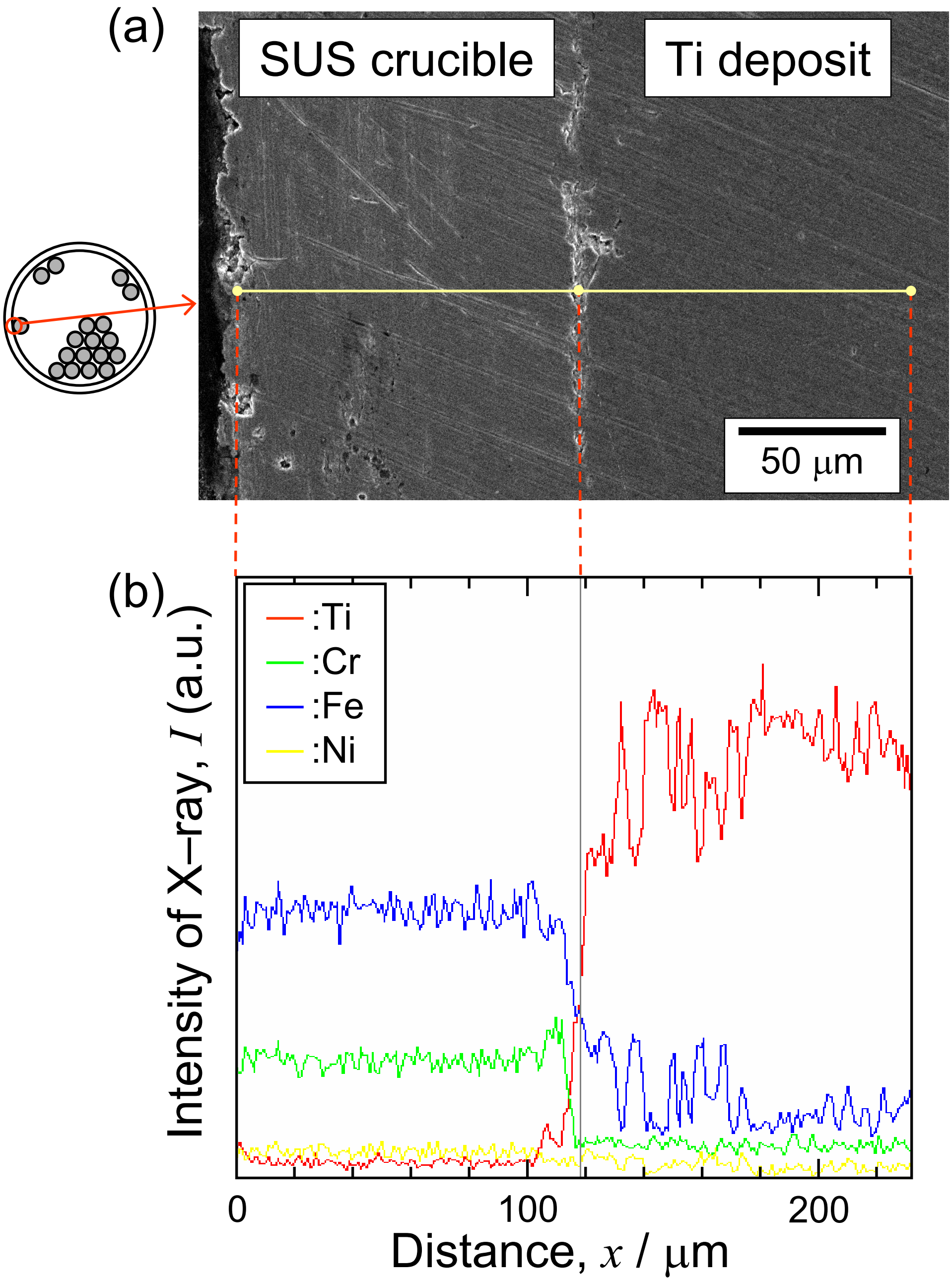

Fig. (a) Scanning electron micrograph of sectioned reduction crucible after the experiment of magnesiothermic reduction of $TiCl_3$. (b) Element concentration profile across the boundary between stainless steel crucible and Ti deposit.

Results, Small Scale, Wet/Dry Separation

(a)

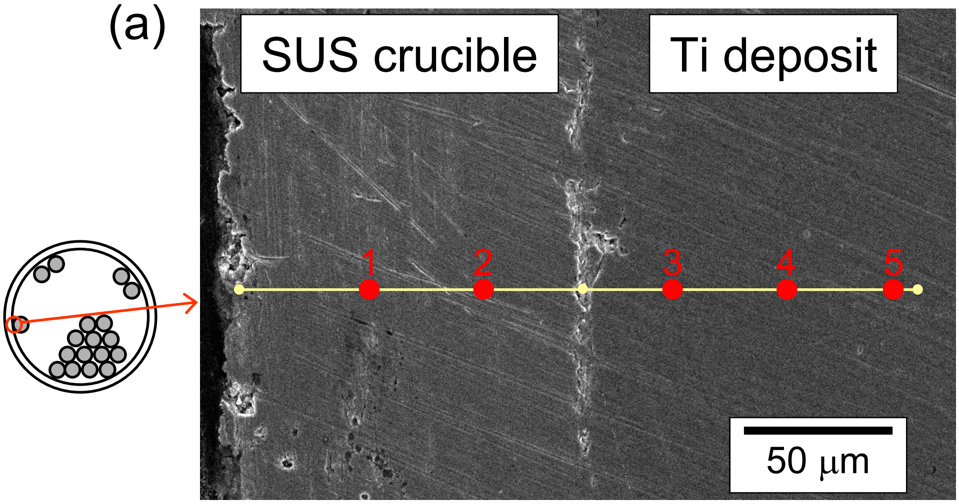

Table Analytical results of point at the boundary between SUS crucible and titanium deposit

Pt.	Concentration of element i, C_i (mass%) [a, b]			
	Ti	Fe	Ni	Cr
1	0.22	72.79	8.33	18.65
2	0.13	72.66	8.83	18.38
3	76.60	14.66	1.69	7.04
4	68.29	22.74	3.77	5.20
5	76.34	15.77	1.49	6.39

Table Analytical results of obtained titanium deposit

Exp.	Concentration of element i, C_i (mass%) [a, b]						Yield
	Ti	Fe	Ni	Cr	Mg	Al	(%)
I	95.79	1.74	0.33	0.36	0.00	0.21	82

Results, Small Scale, Wet/Dry Separation

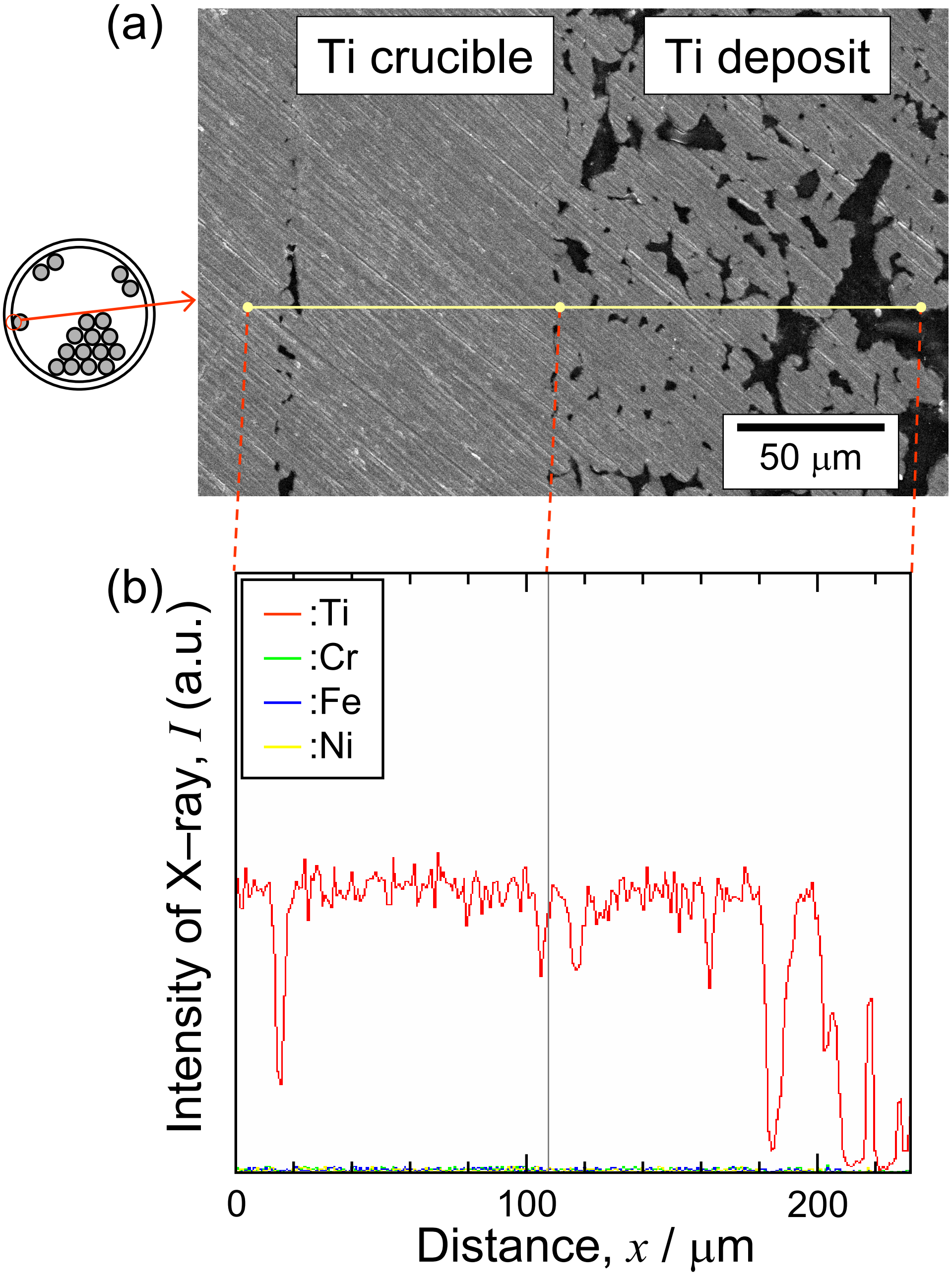

Fig. (a) Scanning electron micrograph of sectioned reduction crucible after the experiment of magnesiothermic reduction of $TiCl_3$. (b) Element concentration profile across the boundary between titanium crucible and titanium deposit (Exp. g).

Results, Small Scale, Wet/Dry Separation

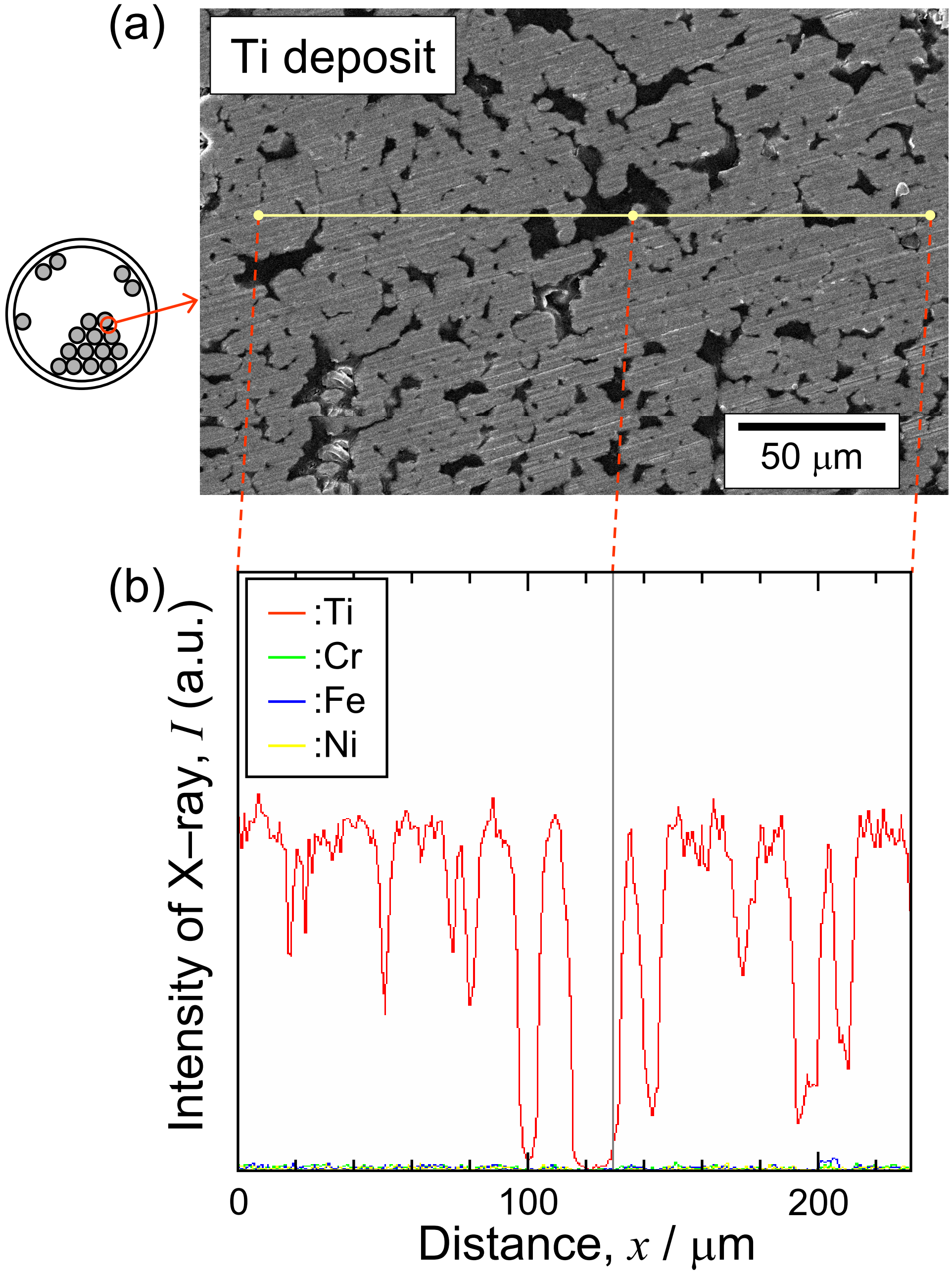

Fig. (a) Scanning electron micrograph of sectioned reduction crucible after the experiment of magnesiothermic reduction of $TiCl_3$. (b) Element concentration profile in a titanium deposit at center of crucible (Exp. g).

Results, Small Scale, Wet/Dry Separation

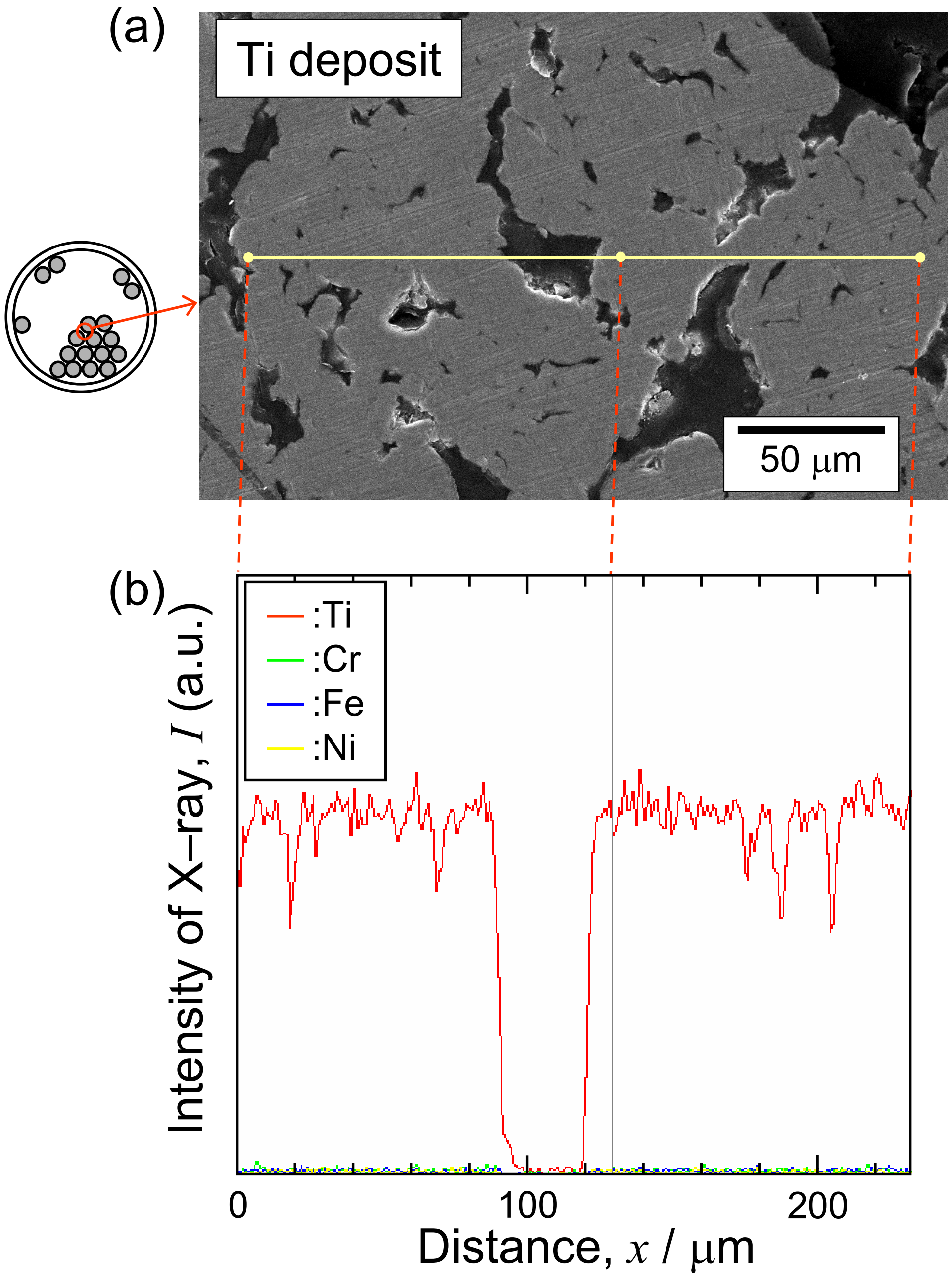

Fig. (a) Scanning electron micrograph of sectioned reduction crucible after the experiment of magnesiothermic reduction of $TiCl_3$. (b) Element concentration profile in a titanium deposit at center of crucible (Exp. I).

Experimental Apparatus, Large Scale, Wet Separation

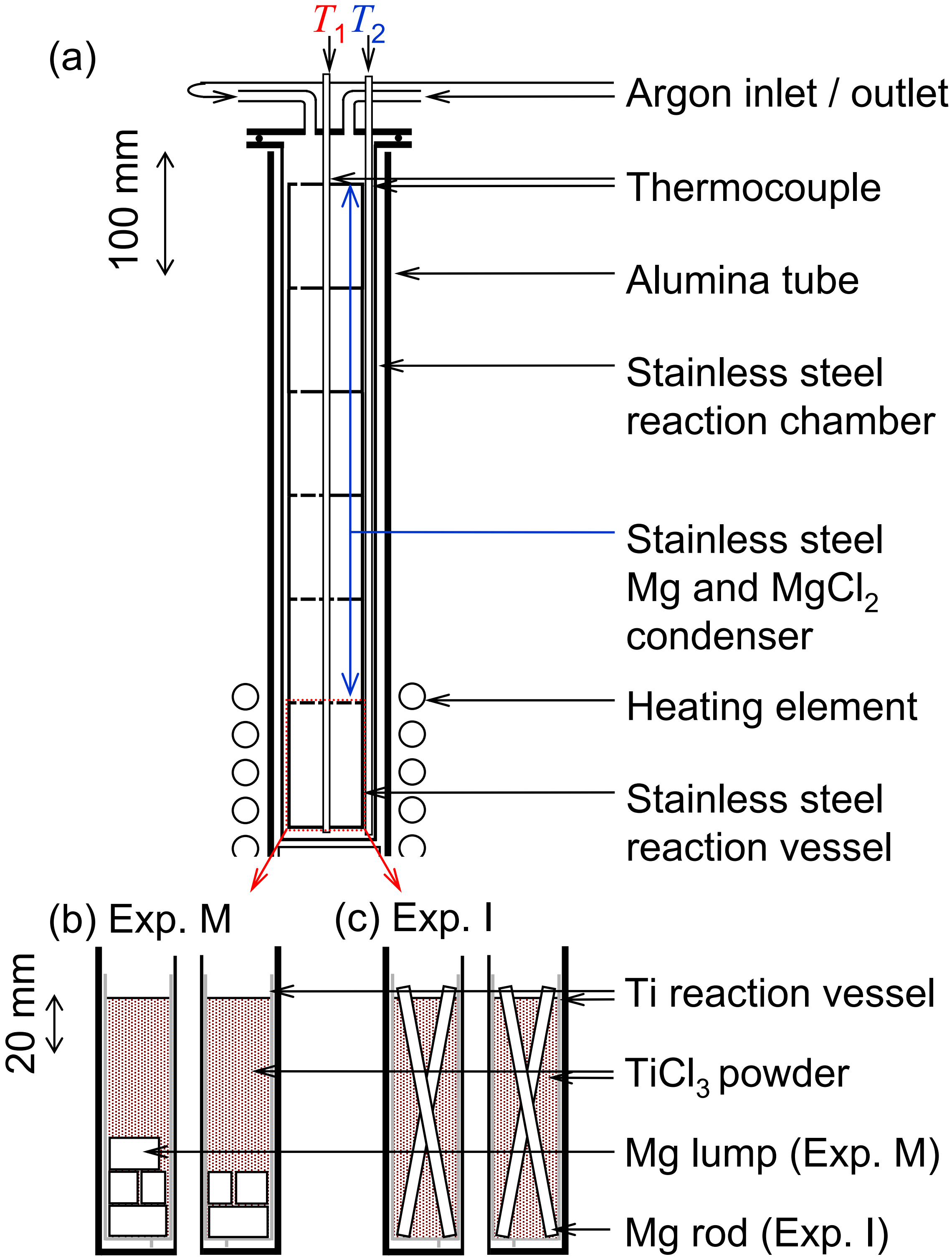

Fig. Schematic illustration of the experimental apparatus for the magnesiothermic reduction of $TiCl_3$, (a) total appearance (b) setup for Exp. M, (c) setup for Exp. I.

Experimental Apparatus, Large Scale, Wet Separation

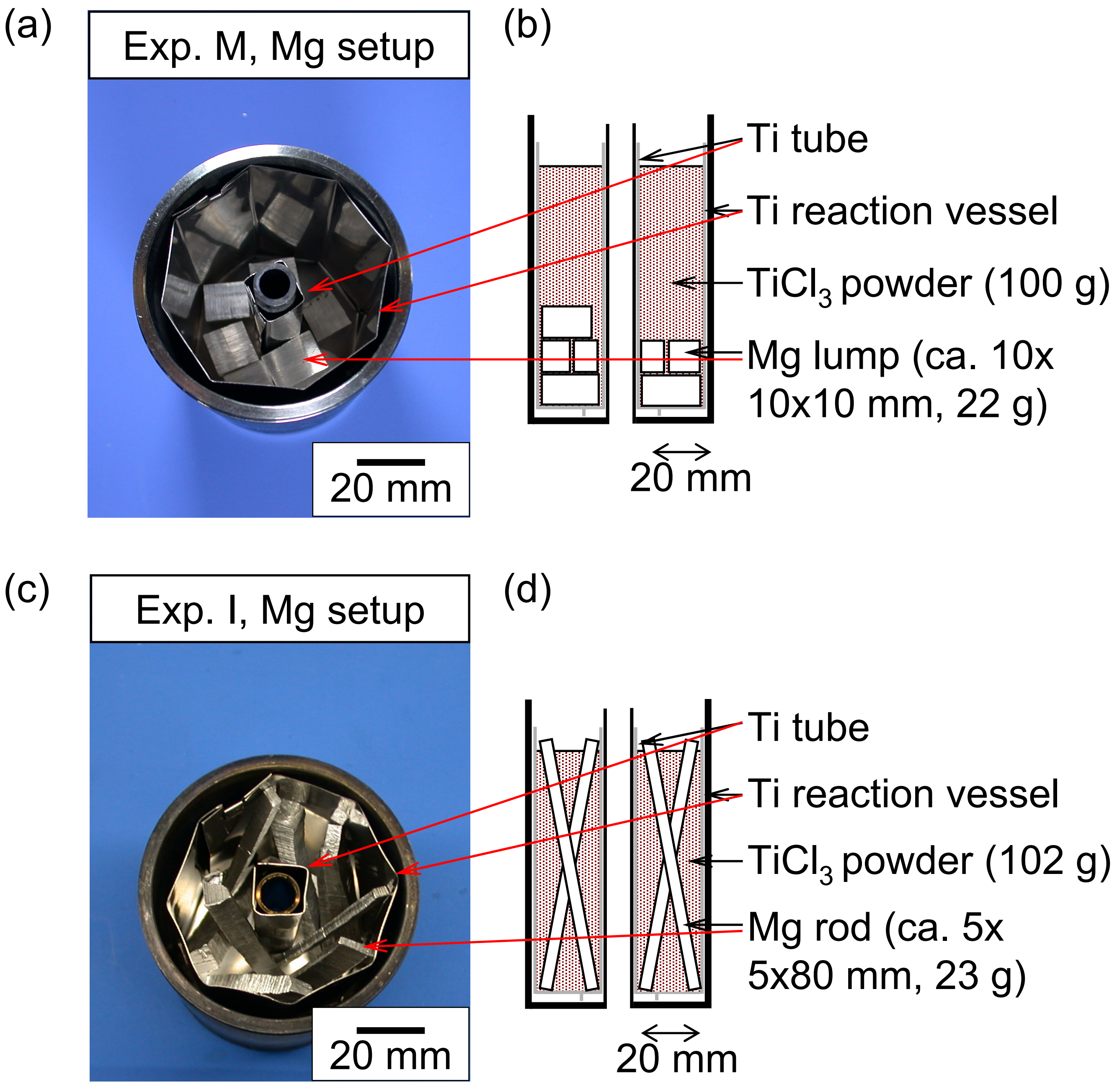

Fig. Photograph and schematic illustration of initial Mg setup before experiment, (a) (b) Exp. M, (c) (d) Exp. I.

Experimental, Large Scale, Wet Separation

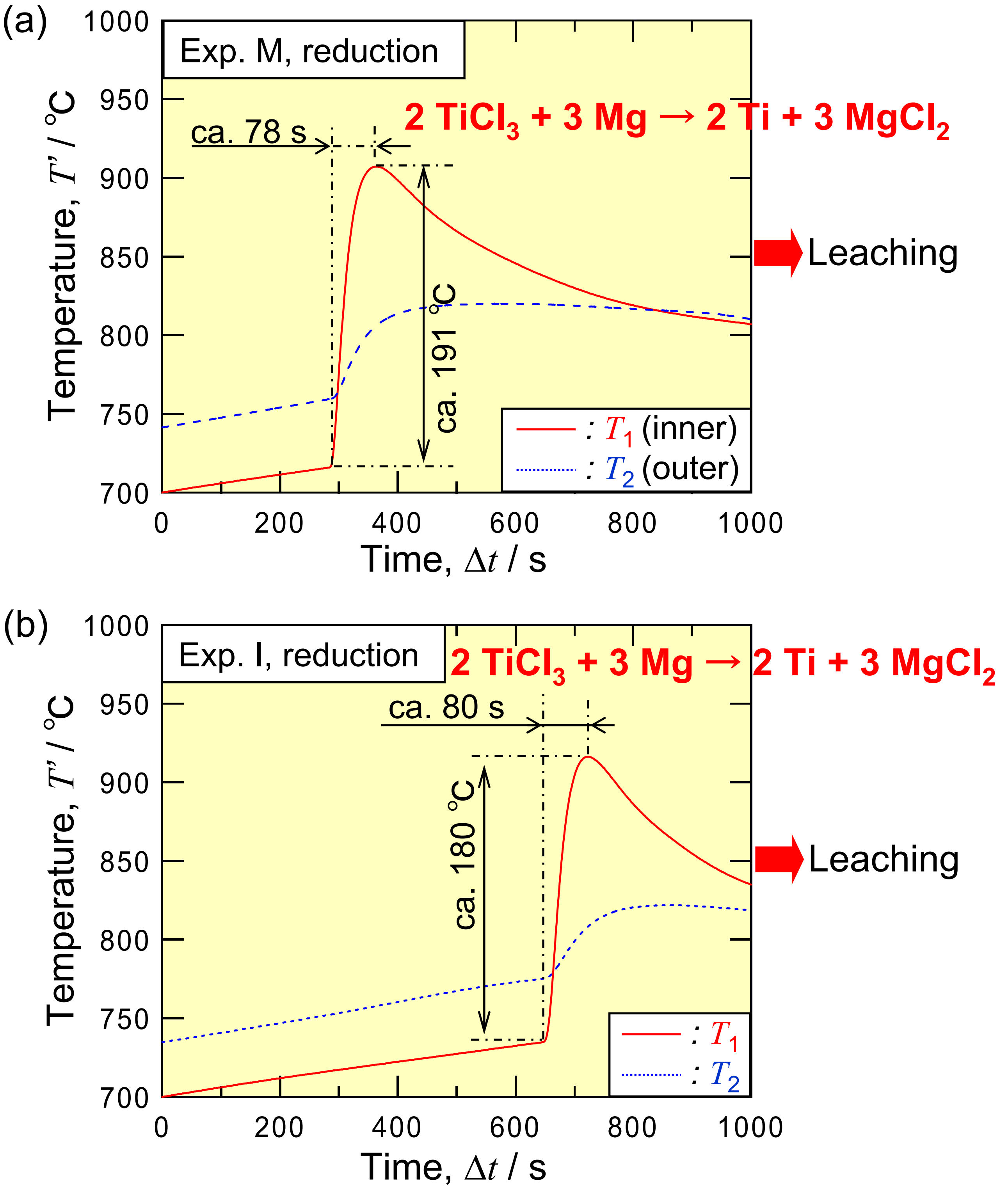

Fig. Transition of sample temperature during experiment of magnesiothermic reduction of $TiCl_3$, (a) Exp. M, (b) Exp. I.

Results, Large Scale, Wet Separation

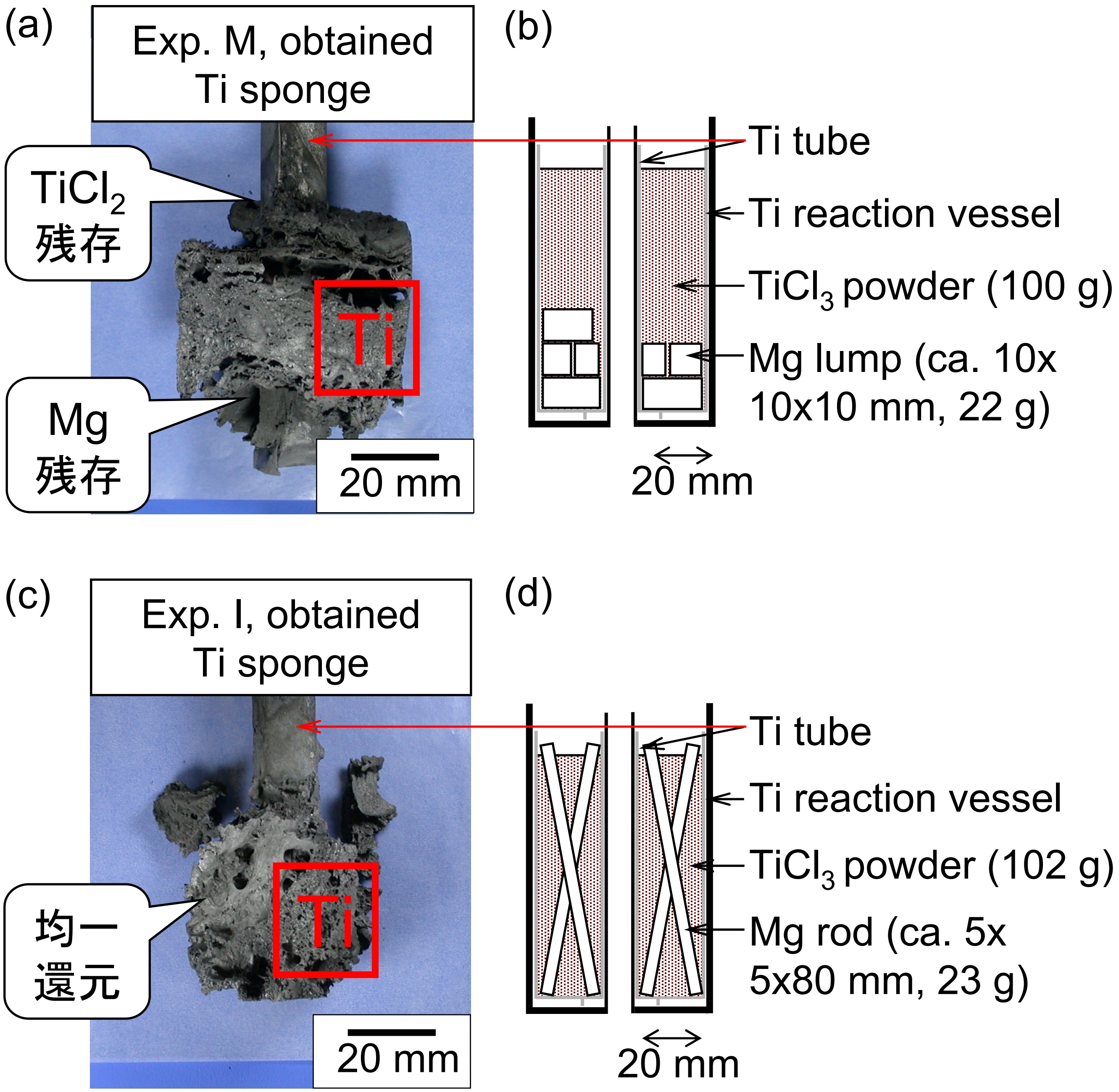

Ti製容器に損傷は見られない

Fig. Photographs of titanium block obtained after the experiment of magnesiothermic reduction of $TiCl_3$ and schematic illustration of initial setup before experiment, (a), (b); Exp. M, (c), (d); Exp. I.

Results, Large Scale, Wet Separation

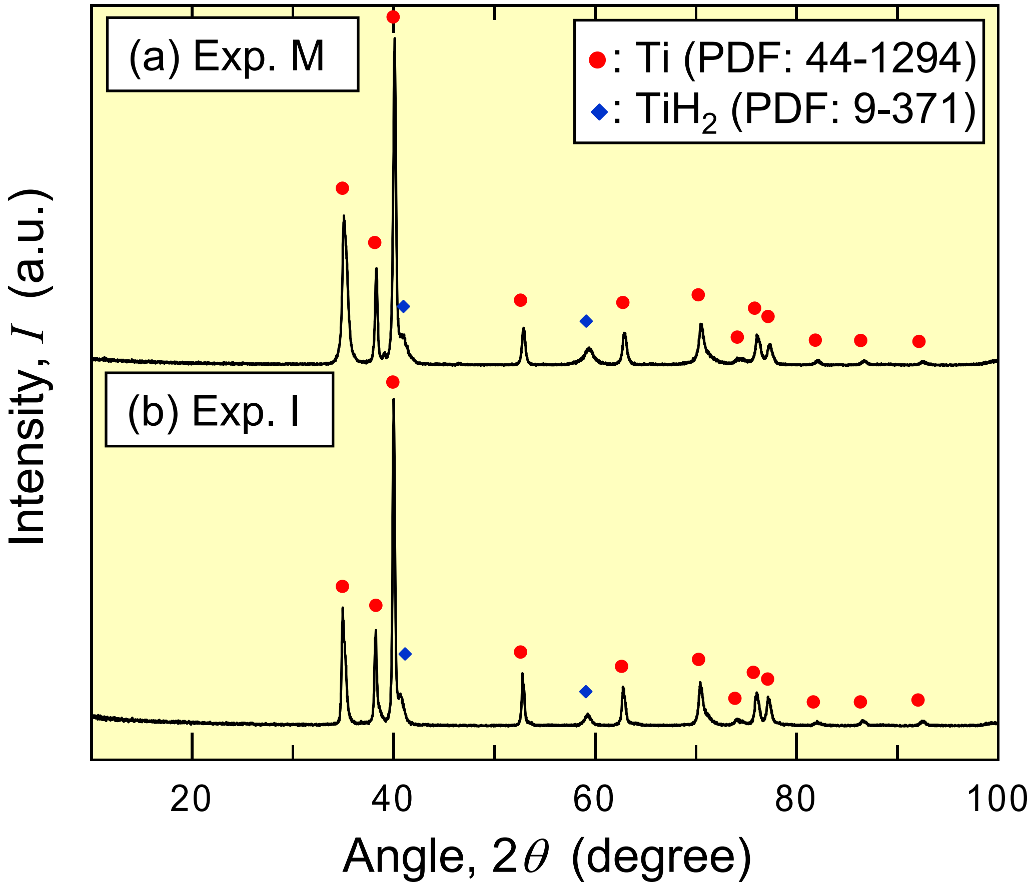

Fig. X-ray diffraction patterns of the obtained samples.

Table
Experimental results for the magnesiothermic reduction of $TiCl_3$

Exp.	Concentration of element i, C_i (mass%) [a, b]						Yield
	Ti	Fe	Ni	Cr	Mg	Al	(%)
M	99.26	0.29	<0.01	<0.01	0.10	0.36	66
I	99.52	0.12	0.01	<0.01	0.11	0.24	91

a: Determined by X-ray fluorescence analysis, and the determined value excludes carbon and gaseous elements.
b: This value is an average of top and bottom in obtained Ti sponge.

Results, Large Scale, Wet Separation

(a)

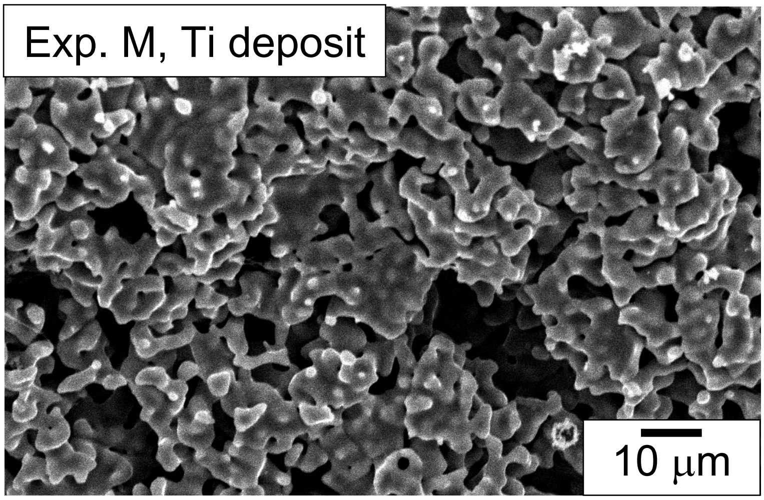

(b)

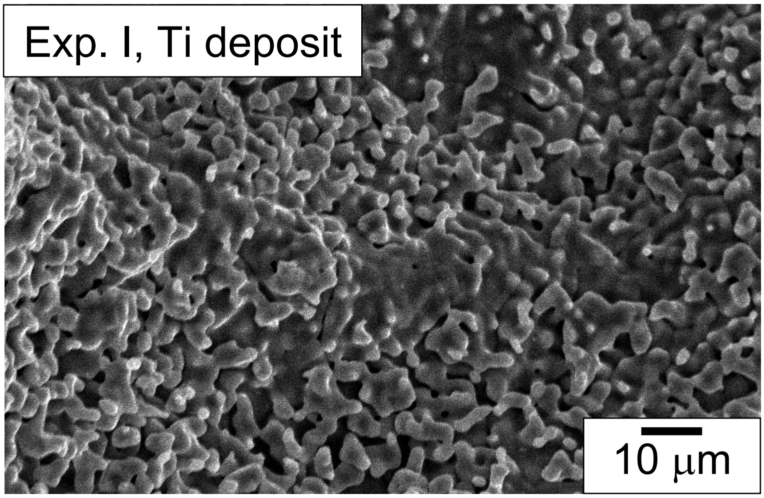

球状の一次粒が結合し、そのネック成長は著しい

Fig. Scanning electron micrograph of Ti sponge after the experiment of magnesiothermic reduction of $TiCl_3$
(a) Exp. M, (b) Exp. I.

Experimental, Large Scale, Dry Separation

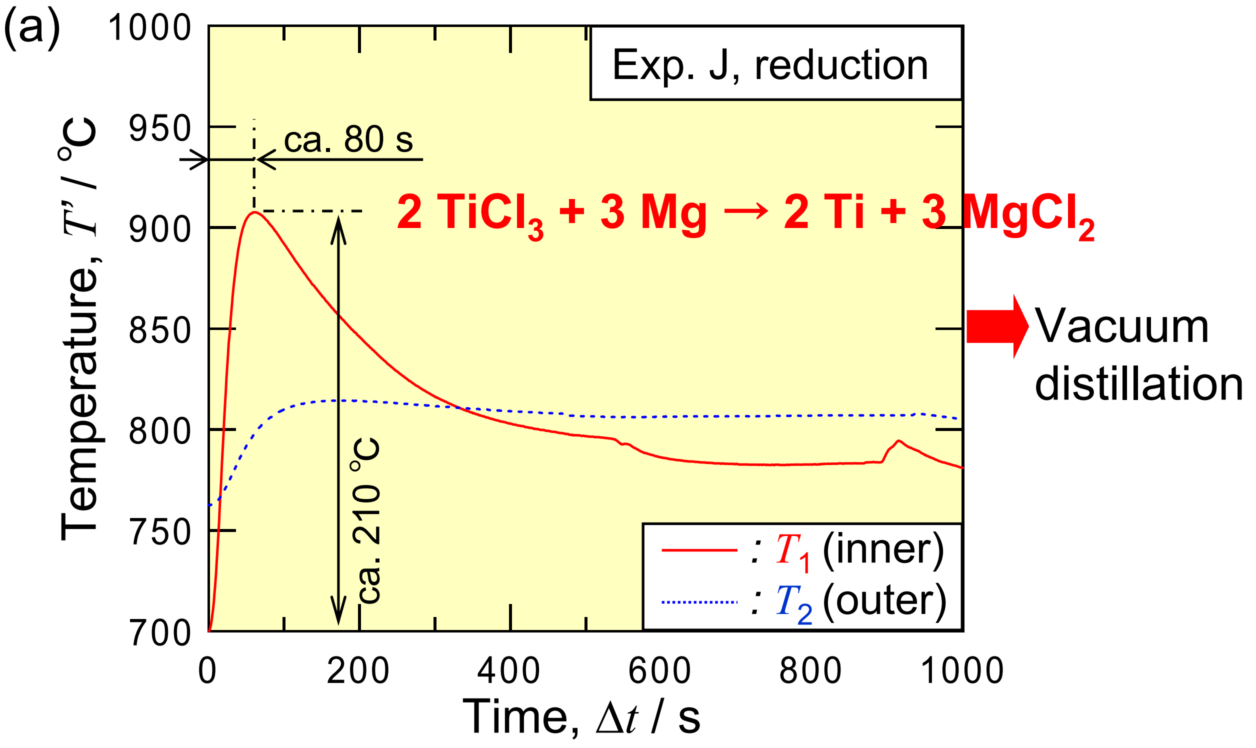

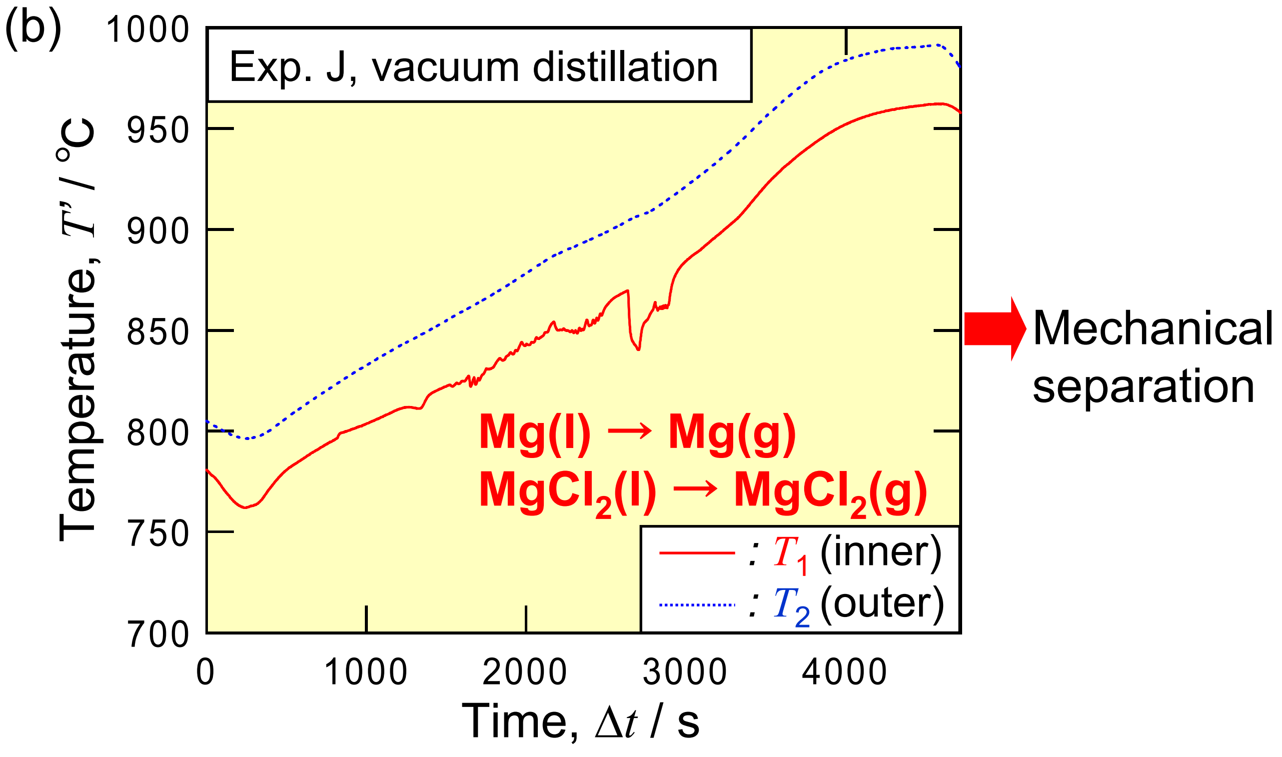

Fig. Temperature change on the experiment of titanium production from $TiCl_3$, (a) reduction, (b) separation (Exp. J).

Results, Large Scale, Dry Separation

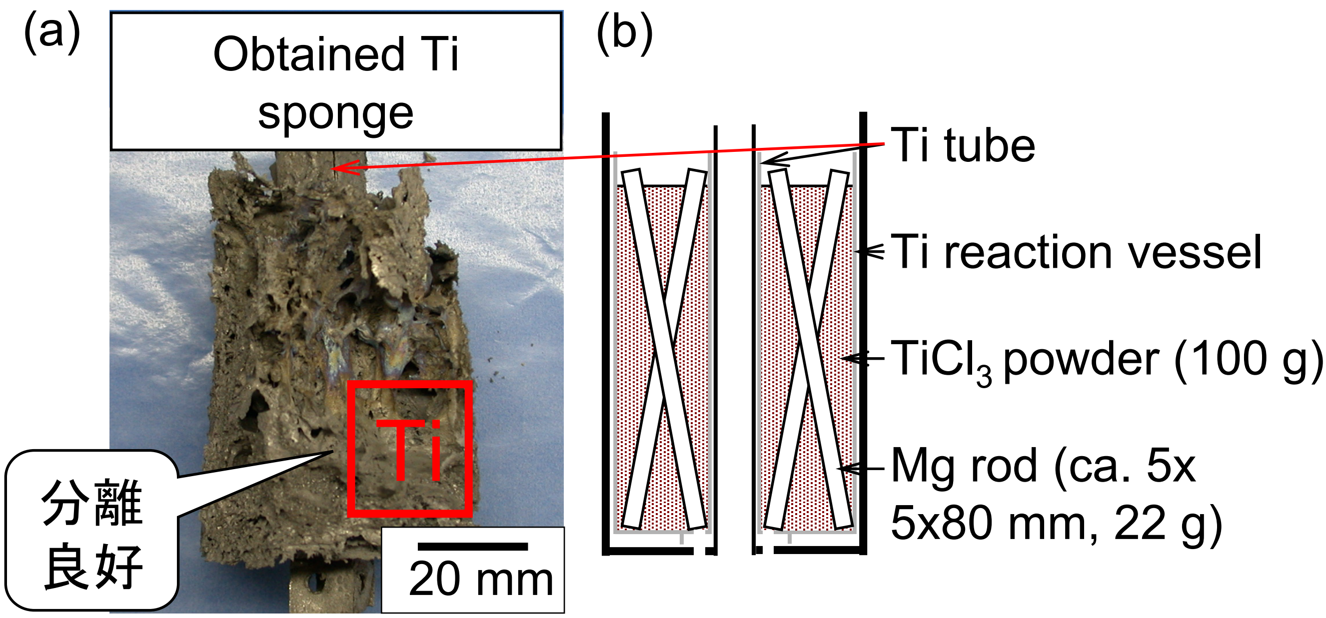

Ti製容器に損傷は見られない

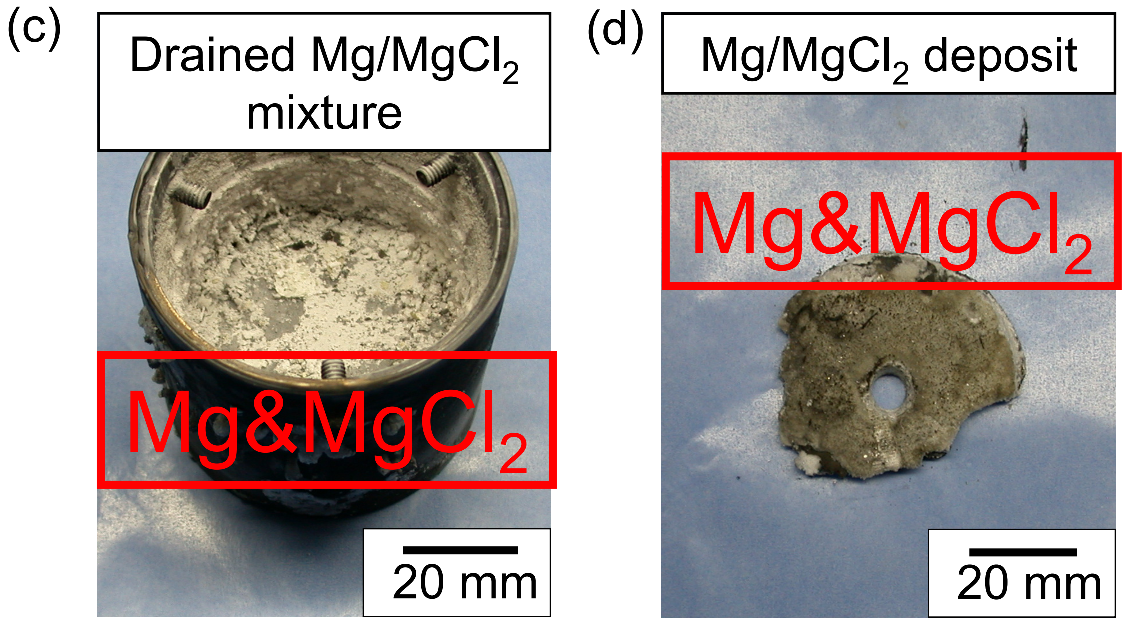

(a) Photograph of obtained Ti sponge after the magnesiothermic reduction of $TiCl_3$,
(b) schematic illustration of initial setup before experiment,
(c) photograph of drained $MgCl_2$ and Mg,
(d) precipitate of $MgCl_2$ and Mg by evaporation (Exp. J).

Results, Large Scale, Dry Separation

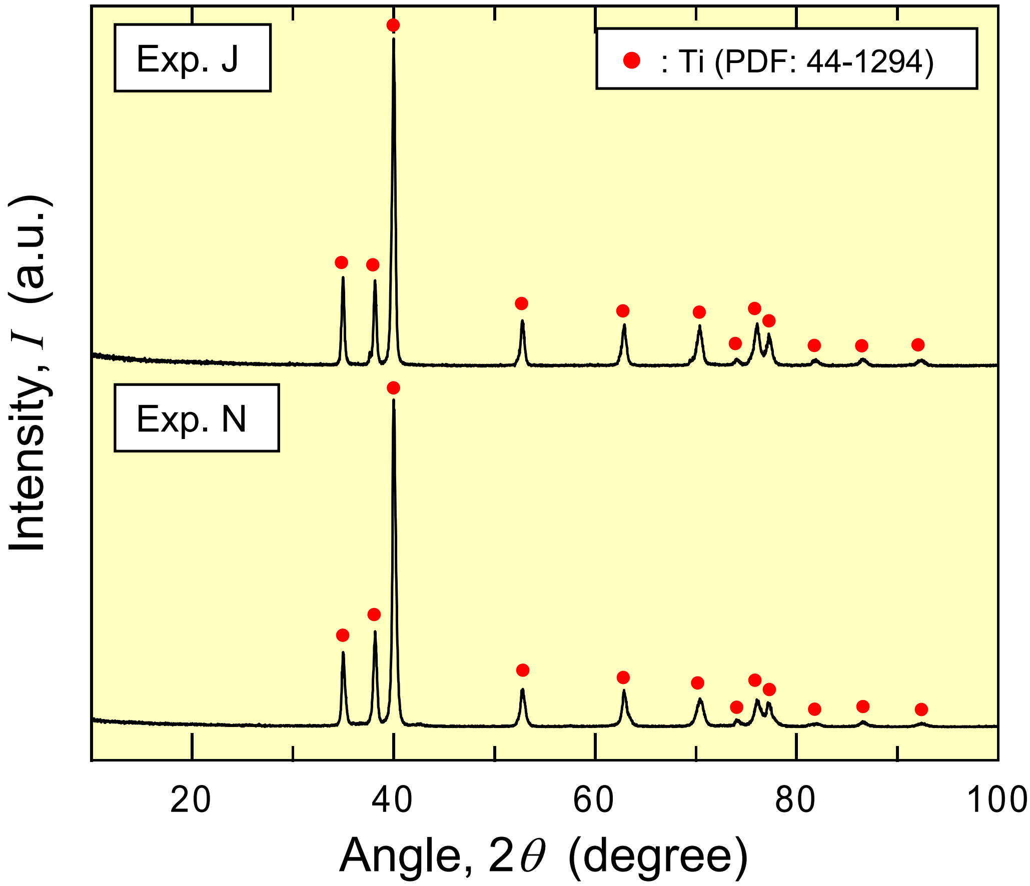

Fig. X-ray diffraction patterns of the obtained sample.

Table
Experimental results for the magnesiothermic reduction of $TiCl_3$

Exp.	Concentration of element i, C_i (mass%) [a, b]						Yield
	Ti	Fe	Ni	Cr	Mg	Al	(%)
J	99.18	0.50	0.01	0.02	0.09	0.21	87
N	99.04	0.18	0.02	0.02	0.09	0.65	82

a: Determined by X-ray fluorescence analysis, and the determined value excludes carbon and gaseous elements.
b: This value is average of top and bottom in obtained Ti sponge.

Results, Large Scale, Dry Separation

(a)
(b)

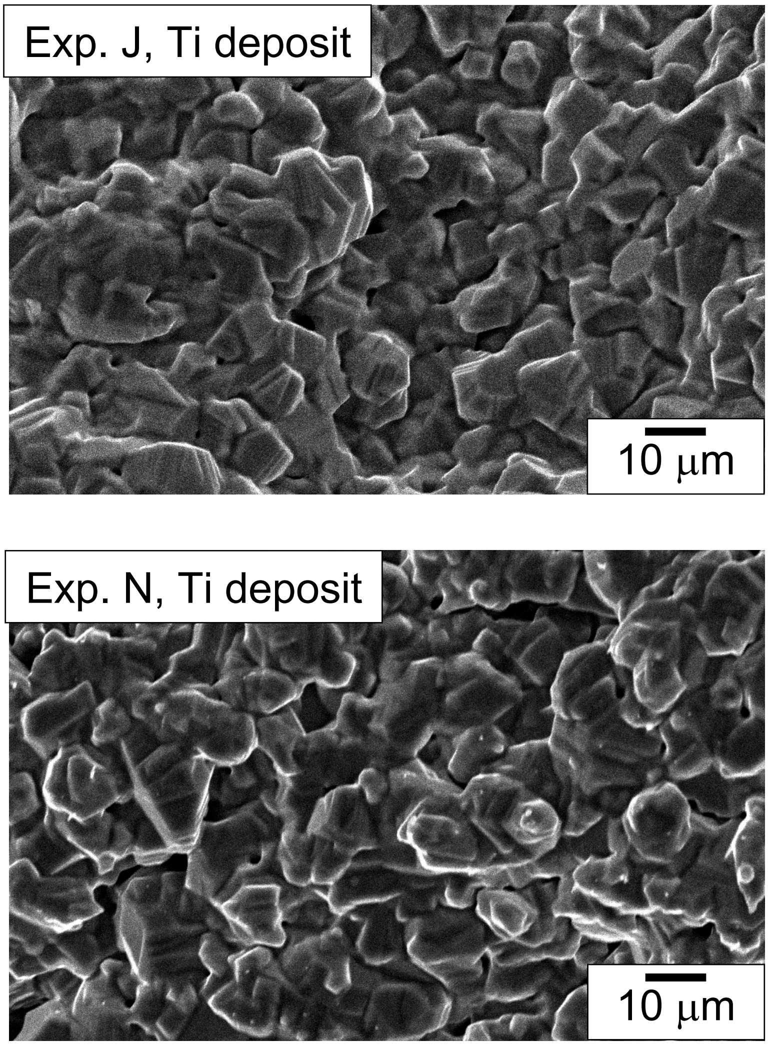

角ばった粗大粒が見られる

Fig. Scanning electron micrograph of Ti sponge after the experiment of magnesiothermic reduction of $TiCl_3$
(a) Exp. J, (b) Exp. N.

Results, Large Scale, Dry Separation

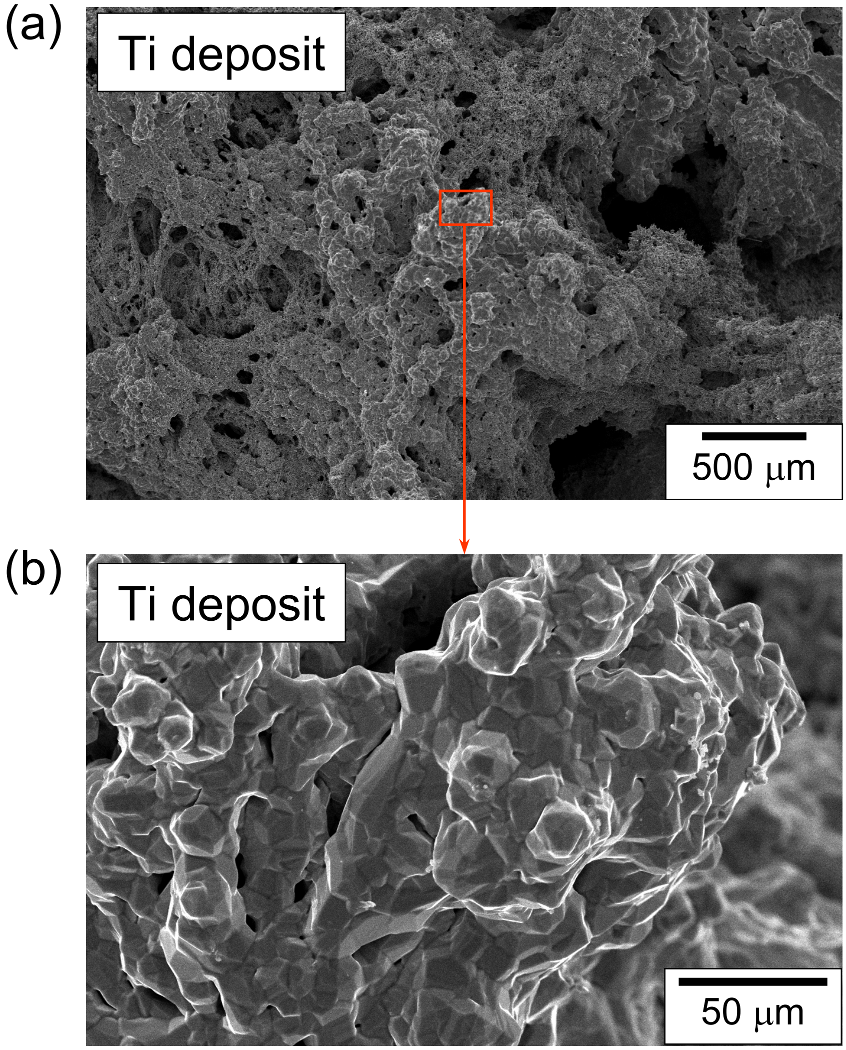

Fig. Scanning electron micrograph of titanium deposit after the experiment of magnesiothermic reduction of $TiCl_3$.

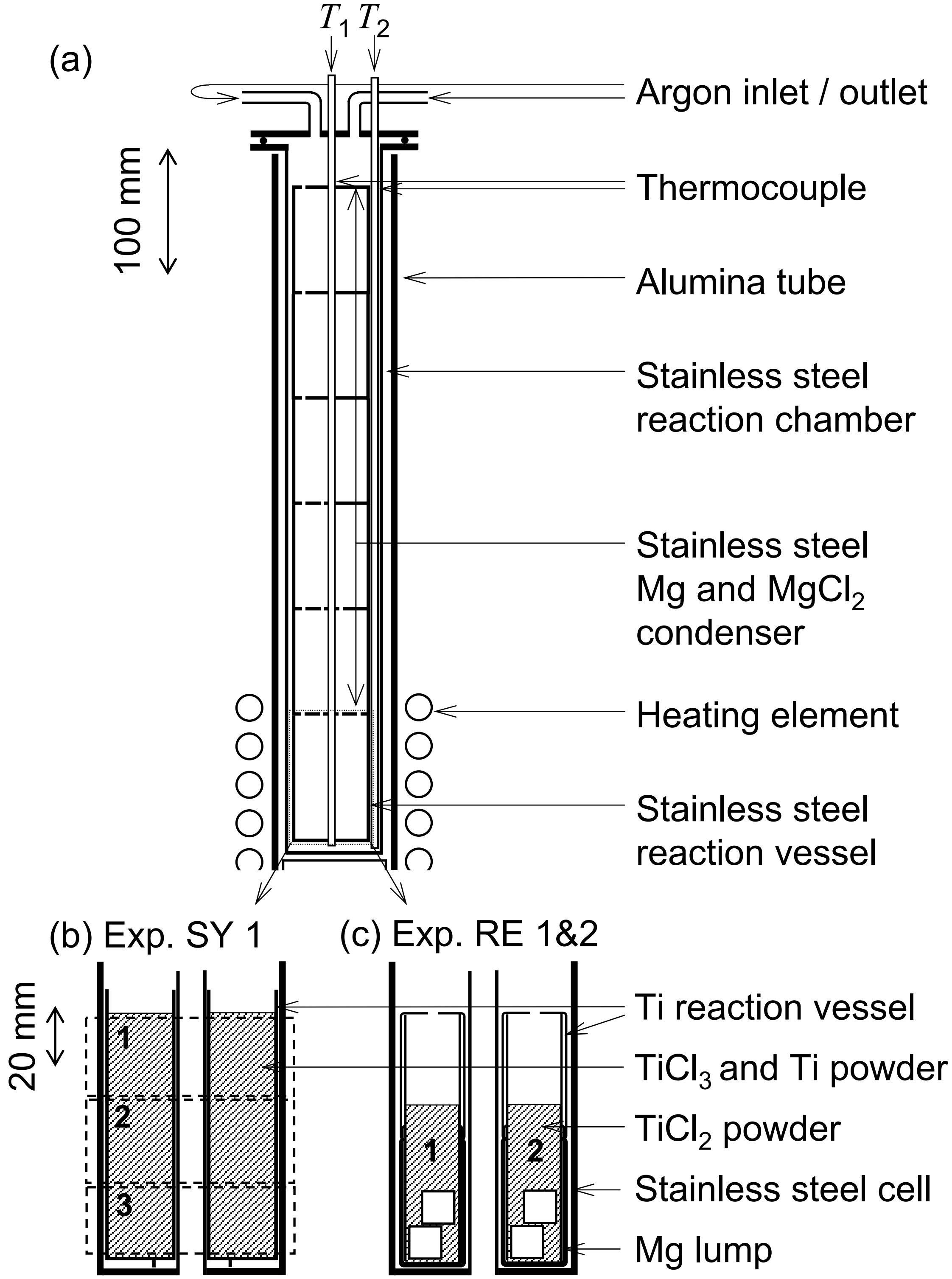

Figure 2. Schematic illustration of the experimental apparatus for the magnesiothermic reduction of $TiCl_2$, (a) total appearance (b) setup for Exp. SY 1, (c) setup for Exp. RE 1&2.

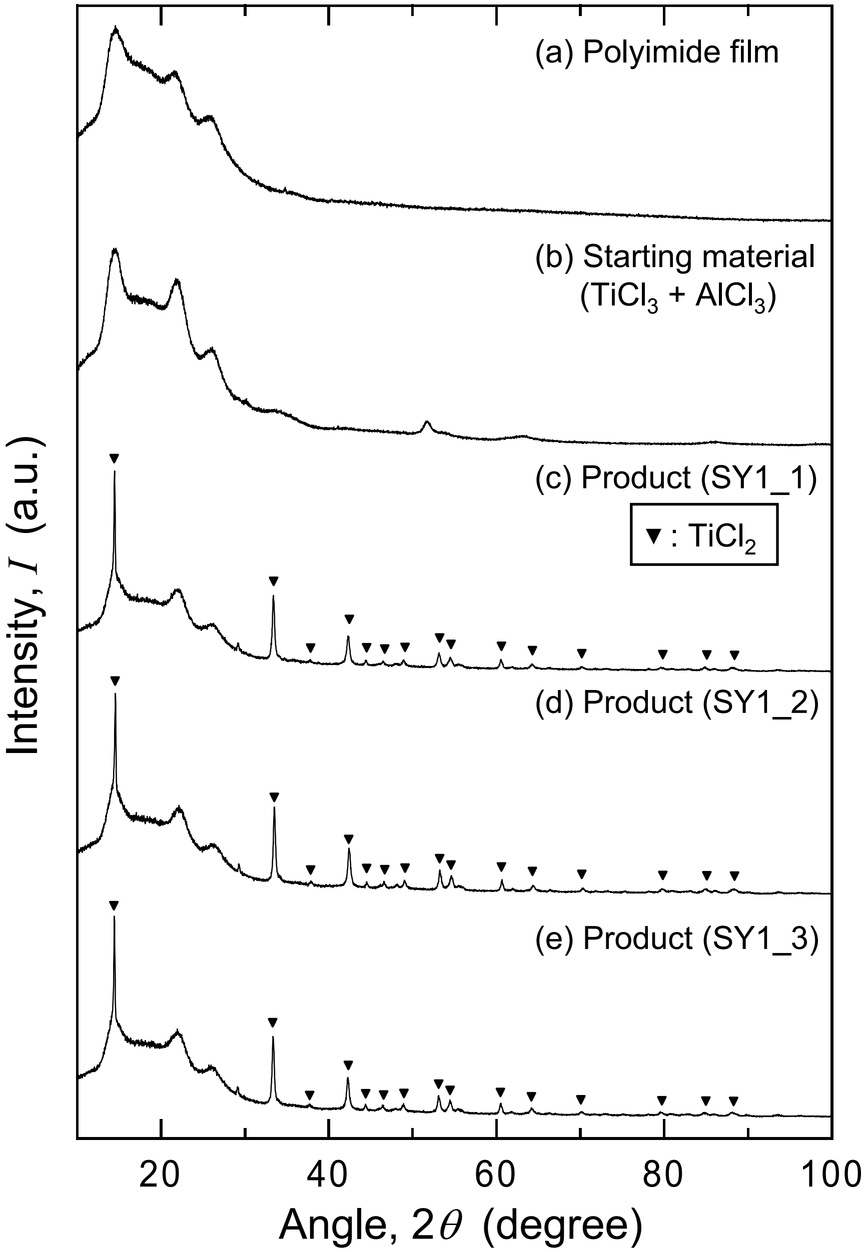

Figure 3. X-ray diffraction patterns of the samples.

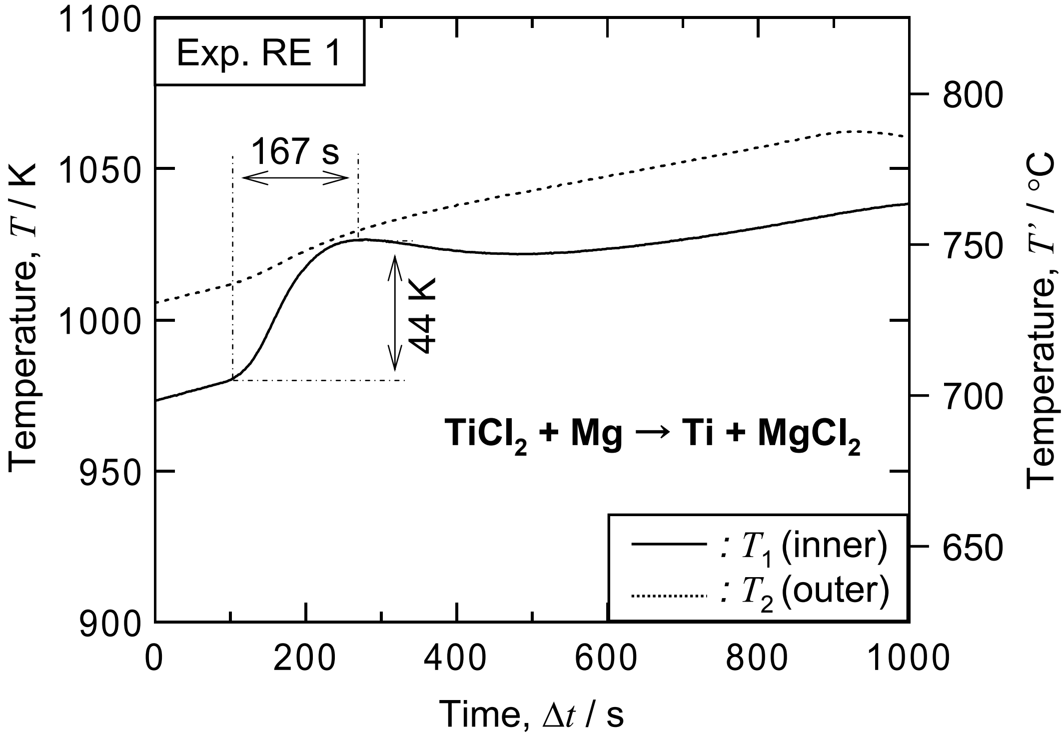

Figure 4. Transition of sampler temperature on experiment of magnesiothermic reduction of $TiCl_2$ [Exp. RE 1].

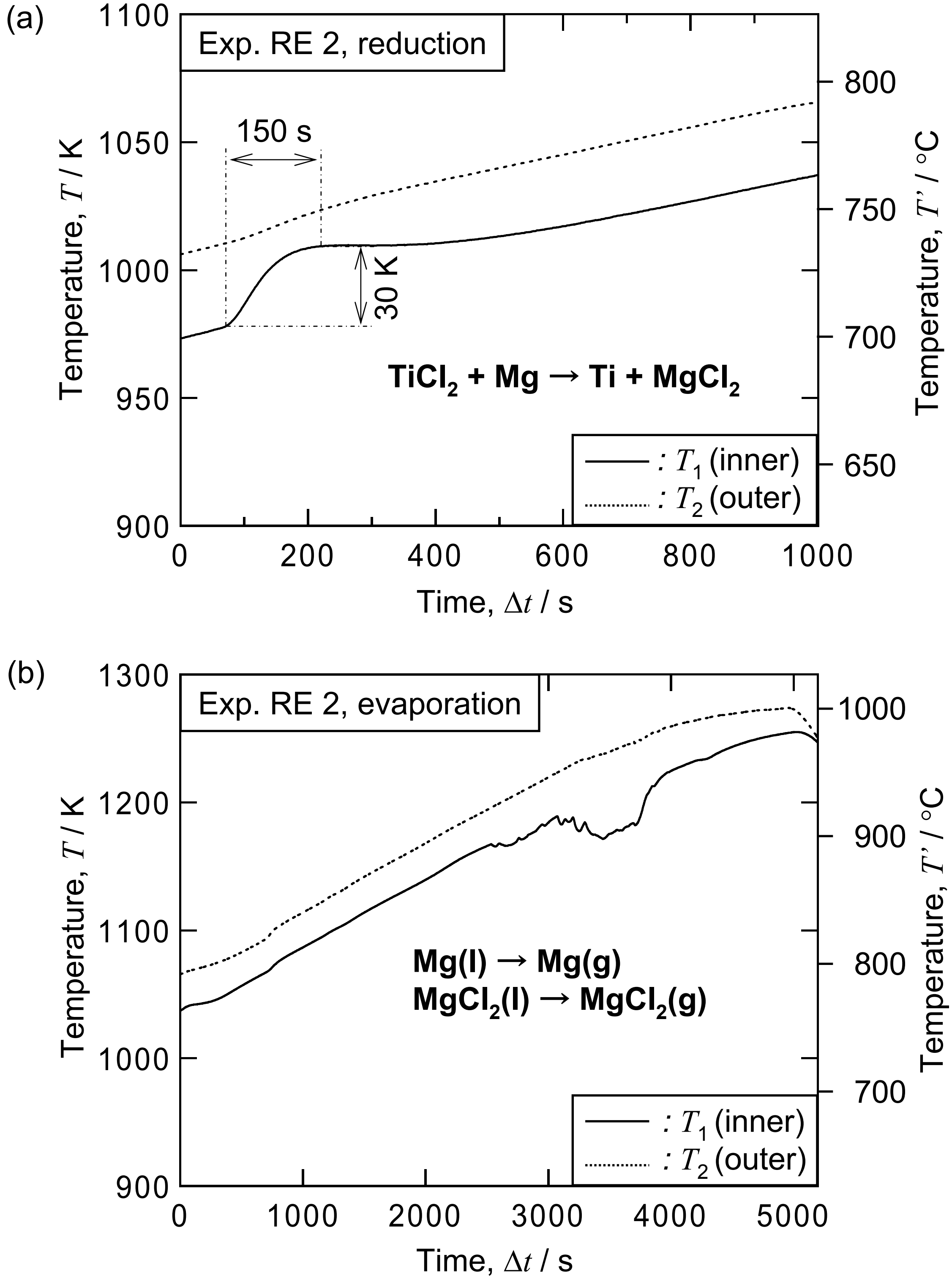

Figure 5. Transition of sampler temperature; (a) on experiment of magnesiothermic reduction of $TiCl_2$, (b) on removal of Mg and $MgCl_2$ from titanium product [Exp. RE 2].

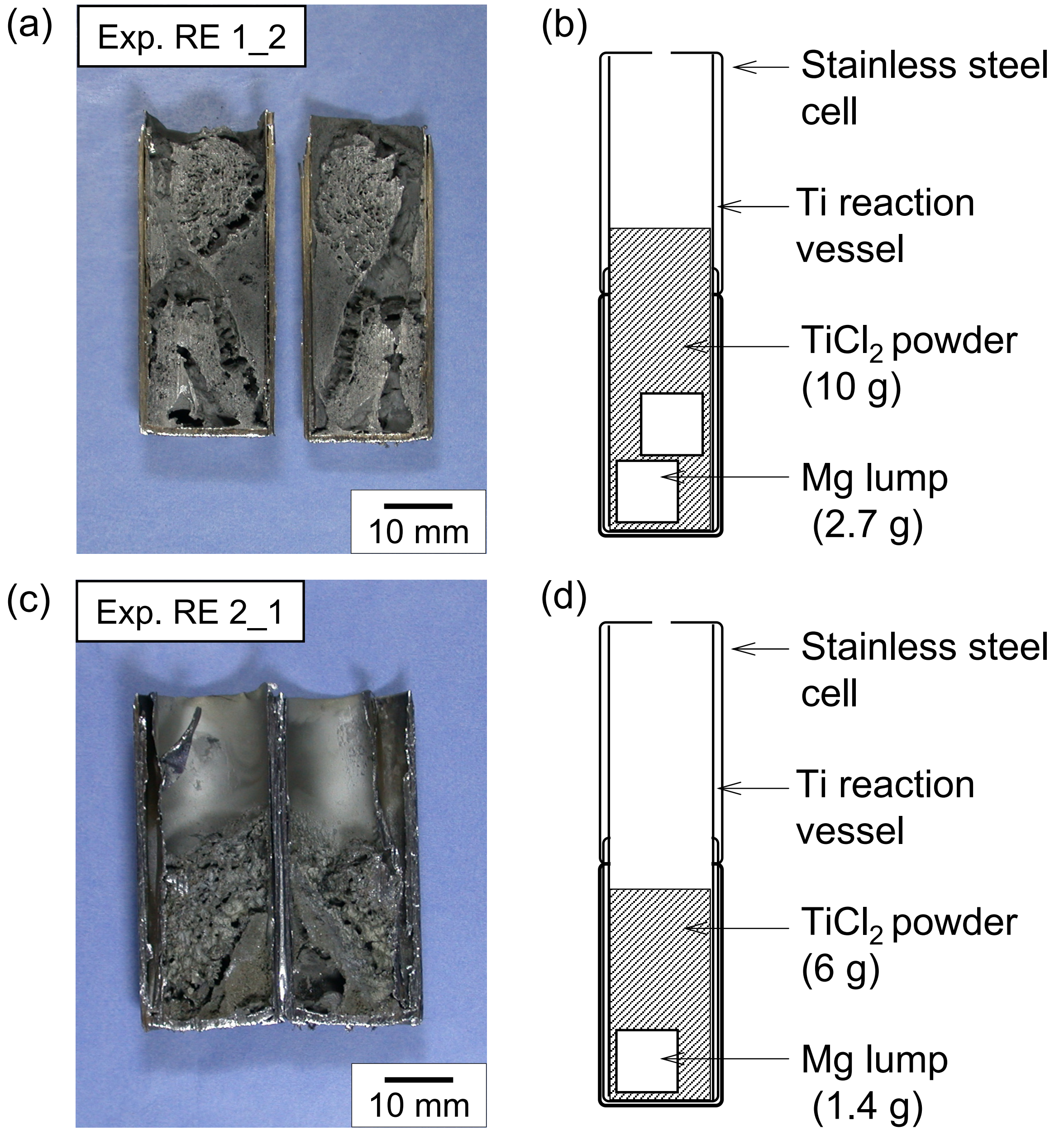

Figure 6. Photograph of sectioned stainless steel capsule after the experiment of magnesiothermic reduction of $TiCl_2$ and schematic illustration of initial setup before experiment, (a) and (b) Exp. RE 1_2, (c) and (d) Exp. RE 2_1.

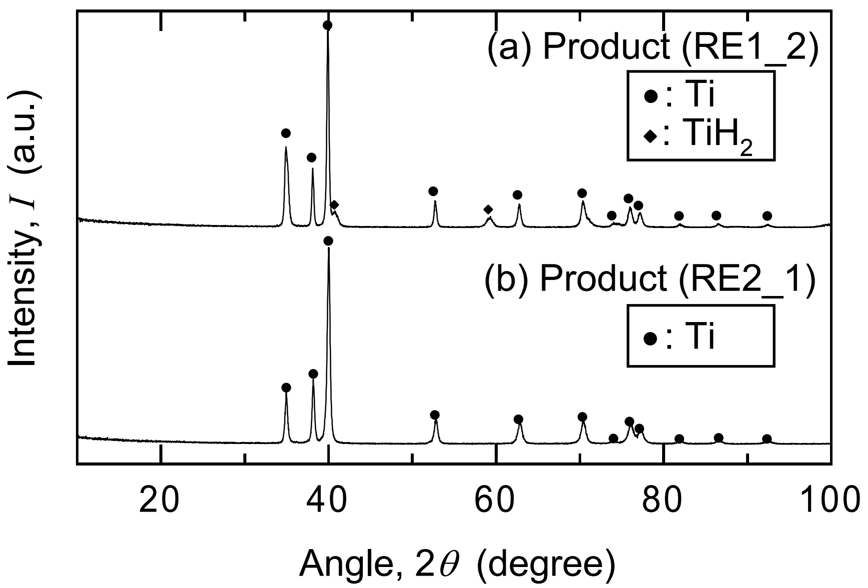

Figure 7. X-ray diffraction patterns of the samples.

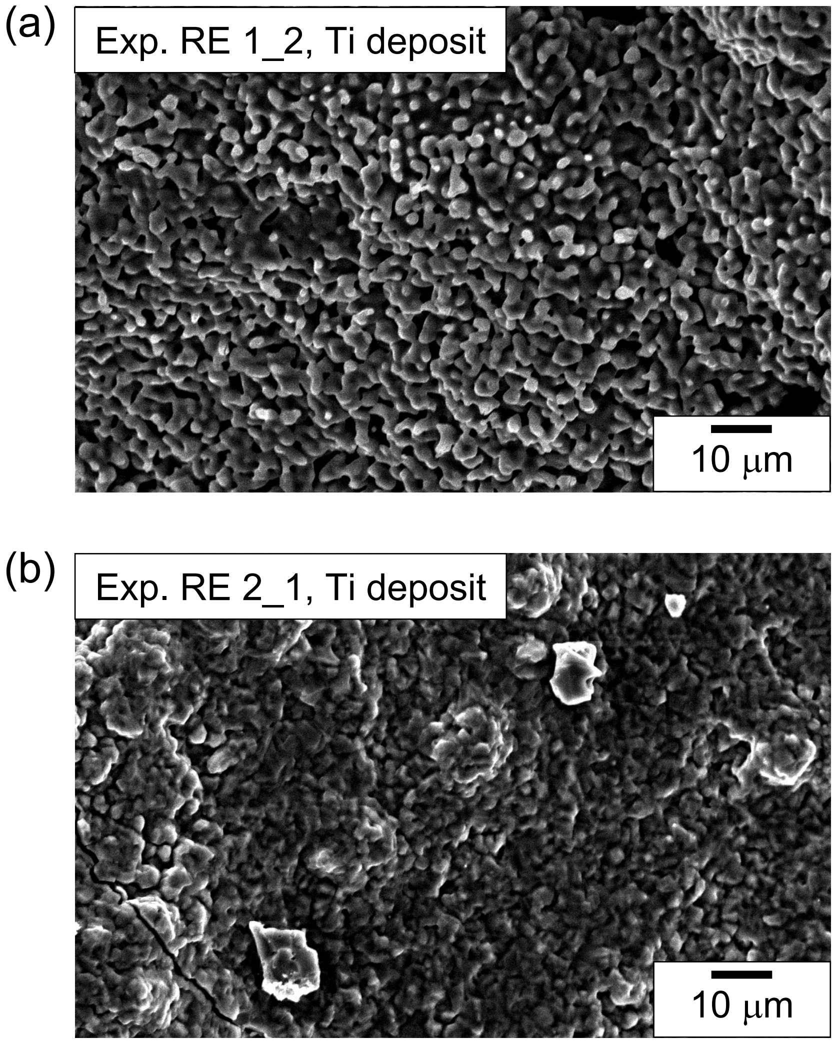

Figure 8 Scanning electron micrograph of Ti sponge after the experiment of magnesiothermic reduction of $TiCl_2$
(a) Exp. RE 1, (b) Exp. RE 2.

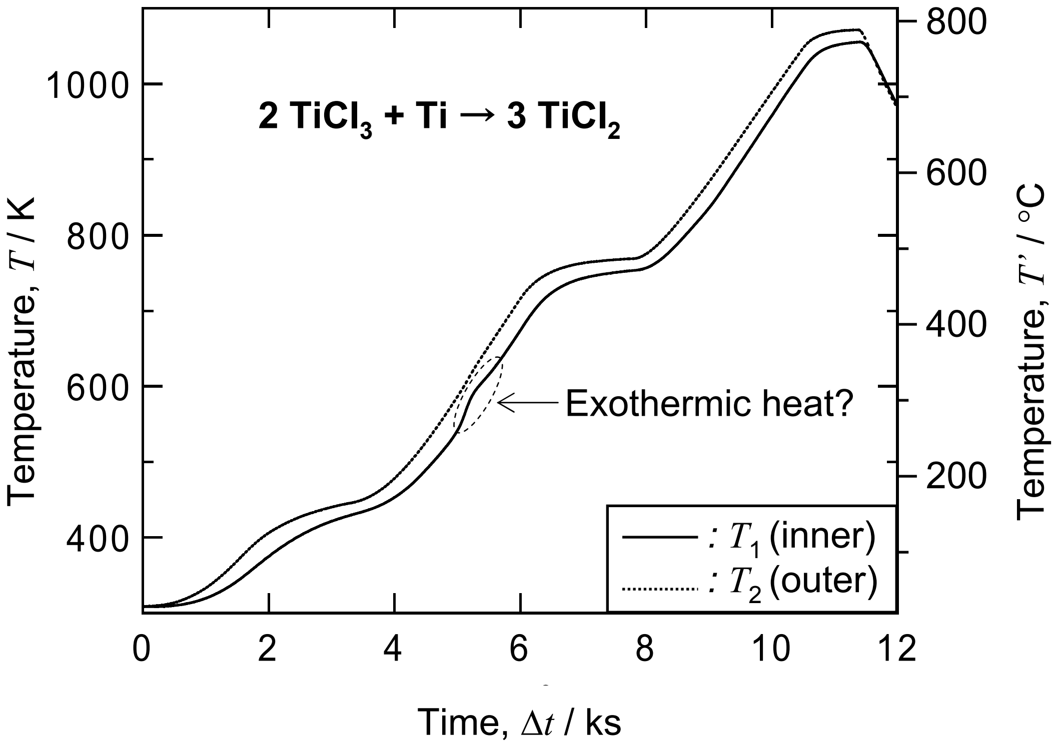

Figure 4. Transition of sampler temperature [Exp. SY1].

(a)

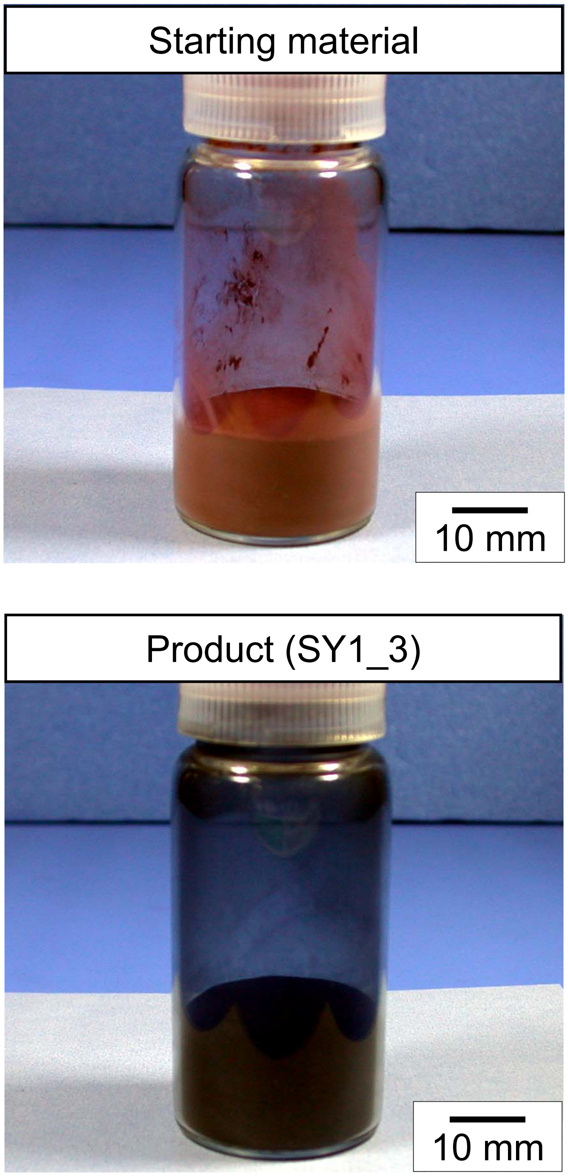

Figure 5. Photograph of powder sample in the experiment of $TiCl_2$ synthesis, (a) starting material ($TiCl_3$ + $AlCl_3$) (b) $TiCl_2$ product (SY1_3).

Results, Appearance of Sample

(a) Sectioned reaction container after reduction (prior to leaching)

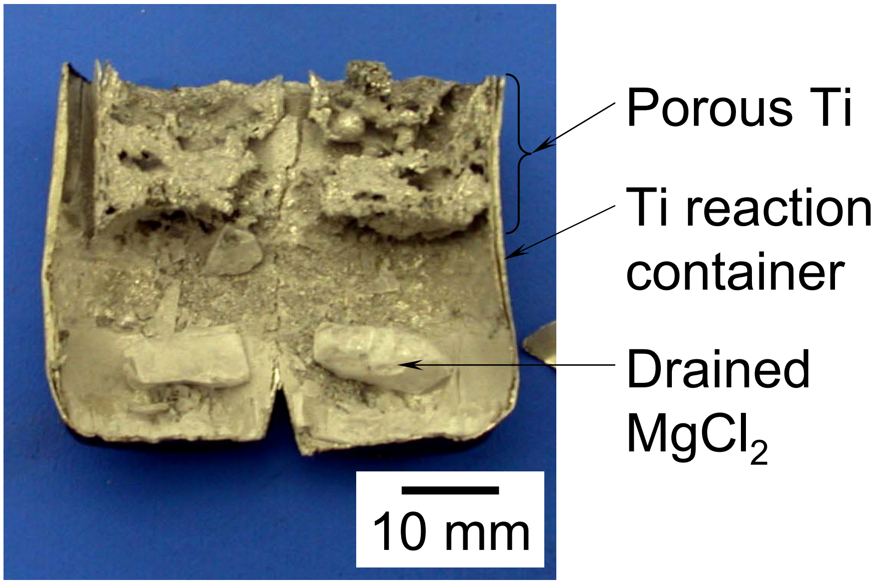

(b) Initial setup of (a)

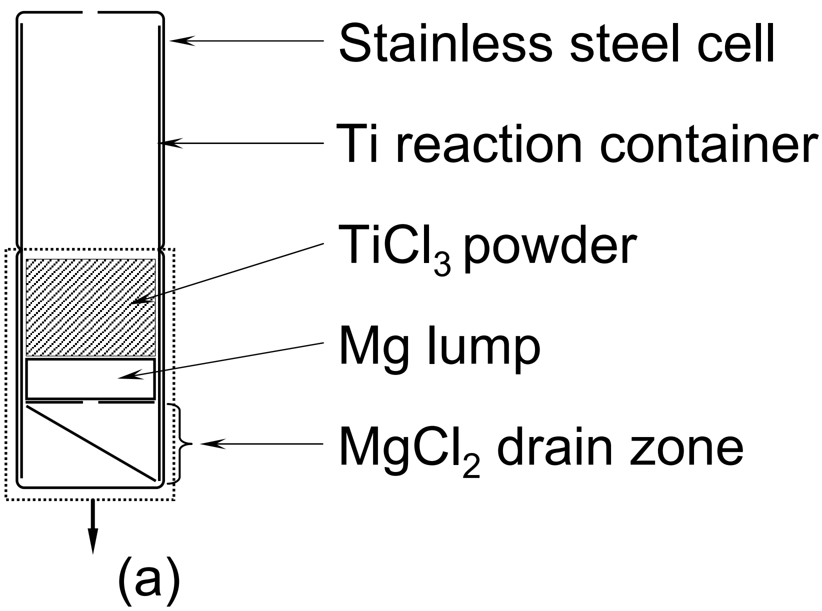

Figure Sectioned titanium reaction container after the experiment for the magnesiothermic reduction of $TiCl_3$: (a) photograph of obtained sample, (b) initial setup of the reaction vessel [A].